

PSFC/RR-00-4

**Effects of Radius, Microwave Power, and  
Gas Flow Rate on the Electronic Excitation  
Temperature in an Atmospheric Pressure  
Microwave Plasma Torch**

Karyn M. Green

May 2000

Plasma Science and Fusion Center  
Massachusetts Institute of Technology  
Cambridge, MA 02139 USA

This work was supported by the U.S. Department of Energy, Mixed Waste Focus Area, Office of Science and Technology, Environmental Management, Grant No. 66576. Reproduction, translation, publication, use and disposal, in whole or in part, by or for the United States government is permitted.

# Effects of Radius, Microwave Power, and Gas Flow Rate on the Electronic Excitation Temperature in an Atmospheric Pressure Microwave Plasma Torch

by

Karyn M. Green

Submitted to the Department of Nuclear Engineering  
on May 5, 2000, in partial fulfillment of the  
requirements for the degrees of  
Master of Science in Nuclear Engineering  
and  
Nuclear Engineer in Nuclear Engineering

## Abstract

The microwave plasma continuous emissions monitor (MP-CEM) utilizes atomic emission spectroscopy to study trace quantities of hazardous metals such as mercury and lead. With the aim of improving the MP-CEM sensitivity to these metals, a series of experiments are performed to characterize this microwave plasma operating at atmospheric pressure. All experiments use air as the working gas.

Assuming local thermal equilibrium, a comparison of the relative emissivity values of single-ionized iron lines yields the electronic excitation temperature,  $T_{exc}$ , of the plasma. While maintaining a constant flow rate of 0.5 cfm, a 55 % increase in microwave power from 900 W to 1400 W leads to  $\sim 100$  % increase in plasma volume. The same increase in microwave power has no effect on the electronic excitation temperature. With a microwave power of 1400 W, an increase in total flow rate from 0.4 cfm to 1.0 cfm decreases the volume of the plasma by  $\sim 25$  % and increases the  $T_{exc}$  by  $\sim 10$  %.

Thesis Supervisor: Paul P. Woskov

Title: Associate Division Head, Plasma Technology Division,  
Plasma Science and Fusion Center

# Acknowledgments

First, I thank Paul Woskov for providing me with intriguing and challenging work on the microwave plasma torch project. Indeed, I thank the entire Plasma Technology Division for providing an enjoyable work atmosphere. I especially thank Cristina Borrás for her endless patience and guidance throughout these experiments. Kamal Hadidi and Paul Thomas have also discussed the plasma torch research with me in detail, and I thank them for giving me insight into many different aspects of the torch. Additionally, I thank Mary Pat McNally for her help with all of my figures.

Even though G.J. Flores III and Brian Pollack have left MIT and the Plasma Technology Division, I have picked their brains numerous times. For taking the time to discuss ideas for the torch, I thank both of them.

As always, I thank my brother, Edward, for instilling in me an intense desire to explore and learn. An especial thanks goes out to my mother, Nancy E. Walker for all of her support, not only during the writing of my thesis, but throughout my life.

The research presented in this text was sponsored by the Mixed Waste Focus Area, Office of Science and Technology, Environmental Management, Department of Energy.

# Contents

<b>1</b>	<b>Introduction</b>	<b>10</b>
1.1	Stationary Emission Monitors . . . . .	10
1.1.1	Method 29 . . . . .	10
1.2	Continuous Emission Monitors . . . . .	11
1.2.1	Inductively-Coupled Plasmas . . . . .	11
1.2.2	Laser Spark . . . . .	13
1.2.3	Microwave Plasmas . . . . .	13
1.3	Outline of Text . . . . .	15
<b>2</b>	<b>Analytical Basis of Measurements</b>	<b>16</b>
2.1	Abel Inversion . . . . .	16
2.2	Local Thermal Equilibrium . . . . .	17
2.3	Electronic Excitation Temperature . . . . .	19
2.4	Plasma Parameters . . . . .	21
2.5	Microwave Parameters . . . . .	24
<b>3</b>	<b>Apparatus</b>	<b>26</b>
3.1	Microwave Plasma Torch System . . . . .	26
3.2	Gas Flow System . . . . .	28
3.3	Sample Injection System . . . . .	30
3.4	Fiber Optics System . . . . .	31
<b>4</b>	<b>Data Collection and Analysis Procedures</b>	<b>33</b>

4.1	Data Collection . . . . .	33
4.1.1	Apparatus Settings . . . . .	33
4.1.2	Scanning the Plasma . . . . .	35
4.2	Data Analysis . . . . .	36
4.2.1	Conversion of Data . . . . .	36
4.2.2	Intensity Measurements . . . . .	38
4.2.3	Emissivity Profiles . . . . .	40
4.2.4	Electronic Excitation Temperature . . . . .	41
<b>5</b>	<b>Results and Discussion</b>	<b>45</b>
5.1	Emissivity Profiles . . . . .	45
5.1.1	Microwave Power Variation . . . . .	45
5.1.2	Gas Flow Rate Variation . . . . .	47
5.2	Electronic Excitation Temperature Profiles . . . . .	47
5.2.1	Microwave Power Variation . . . . .	48
5.2.2	Gas Flow Rate Variation . . . . .	49
5.3	LTE Verification . . . . .	52
5.4	Skin Depth and Conductivity Calculations . . . . .	53
<b>6</b>	<b>Future Work</b>	<b>55</b>
<b>A</b>	<b>Electric Field Concentration</b>	<b>58</b>
<b>B</b>	<b>Procedure for Starting the MPT</b>	<b>59</b>
<b>C</b>	<b>Spyglass Macro</b>	<b>61</b>
<b>D</b>	<b>Excel Macro - Water Subtraction</b>	<b>64</b>
<b>E</b>	<b>Excel Macro - Pixel Determination</b>	<b>68</b>
<b>F</b>	<b>Derivations</b>	<b>96</b>
F.1	Radial Emissivity . . . . .	96
F.2	Reconstructed Intensity . . . . .	97

G Excel Macro - Intensity Reconstruction

98

Bibliography

102

# List of Figures

2.1	Geometry for Abel inversion. . . . .	16
3.1	Microwave plasma torch system. . . . .	27
3.2	Gas flow system. . . . .	29
3.3	Sample injection system. . . . .	31
3.4	Optics system. . . . .	32
4.1	Schematic of scanning the plasma. . . . .	35
4.2	Typical atomic iron (Fe I) spectrum. . . . .	37
4.3	Degradation curve of quartz cylinder. . . . .	38
4.4	Typical intensity profile. . . . .	39
4.5	Typical emissivity profile. . . . .	41
4.6	Comparison of numerically reconstructed intensity, $I(y)_{rec}$ , and original intensity, $I(y)$ . . . . .	42
4.7	Determination of electronic excitation temperature. . . . .	42
4.8	Electronic excitation temperature profile. . . . .	43
4.9	Flow chart of data collection procedure. . . . .	44
4.10	Flow chart of data analysis procedure. . . . .	44
5.1	Normalized emissivity at constant flow rate with varying power for a representative Fe I transition. . . . .	46
5.2	Normalized emissivity at constant power with varying flow rate for a representative Fe I transition. . . . .	48

5.3	Electronic excitation temperature at constant flow with varying microwave power. . . . .	49
5.4	Electronic excitation temperature at constant microwave power with varying total gas flow rate. . . . .	51



# List of Tables

1.1	MP-CEM hazardous metals detection limits [34]. . . . .	14
2.1	Fe I emission lines of interest [3]. . . . .	20

# Chapter 1

## Introduction

Since the advent of the Industrial Revolution, factories, furnaces, and incinerators have released their waste products into the atmosphere. During the course of the last century, these facilities have emitted tons of metals and other byproducts into the environment. The effects of metal byproduct emission on the health of populations near furnaces and other facilities have necessitated emissions monitoring.

### 1.1 Stationary Emission Monitors

Presently, hazardous metals emissions fall under government regulation. Some of the regulated metals include arsenic (As), beryllium (Be), mercury (Hg), cadmium (Cd), chromium (Cr), and lead (Pb) [10]. The legal level of emissions for these metals has lowered as the technology to measure the metals and the technology to determine the biological effects of the metals has improved.

#### 1.1.1 Method 29

The Environmental Protection Agency (EPA), the government agency charged with monitoring atmospheric emissions, uses a sampling test called Method 29 to determine a facility's compliance with emission regulations. The Code of Federal Regulations, 40 CFR 60 Part A contains the full details of Method 29, Determination of Metals

Emissions from Stationary Sources [9].

Method 29 requires drawing an isokinetic exhaust stream sample through a filter chain. These filters trap the hazardous metals. Once removed from the exhaust stream of a facility, these filters travel to a laboratory for analysis. In a few days or weeks, the facility will know the average quantity of hazardous metals released into the environment. Since Method 29 requires sending filters off-site for analysis, using this method to prevent the release of excess amounts of hazardous metals is not possible.

Additionally, the EPA has set new, lower limits on the allowable emissions of the hazardous metals, As, Be, Cd, Cr, Hg, and Pb [10]. Method 29, however, cannot provide reliable detection of the metals at the new EPA emission limits.

## **1.2 Continuous Emission Monitors**

The EPA has, therefore, endeavored to develop a method which will in real-time detect low-level emissions of hazardous metals. Under the auspices of the Department of Energy (DOE) Waste Management Program, a DOE division collaborating with the EPA, several experiments have received funding to develop a Continuous Emission Monitor (CEM).

### **1.2.1 Inductively-Coupled Plasmas**

The experiments, funded by the DOE, at ADA Technologies, Battelle, and Morgantown Energy Technology Center use inductively-coupled plasmas (ICPs) to excite the hazardous metals [30]. ICPs operate at radiofrequencies ranging from 0.3 MHz to 70 MHz. The input power regime varies greatly among ICP systems from 0.5 kW to 1.0 MW [5]. Despite the wide fluctuation in operating regimes, most ICPs have similar construction.

The typical ICP consists of three concentric tubes surrounded by induction coils. The number of water-cooled, induction coils depends on the system and the radiofrequency used.

Water or air cools the plasma-confinement tube, the outer tube which is typically a quartz cylinder. A high velocity gas, typically argon, flows between the plasma confinement tube and the intermediate tube [5]. This gas flow prevents the plasma from overheating the outer tube.

The intermediate tube, constructed of quartz or metal, extends to the first induction coil [5]. The intermediate tube carries the plasma gas, which prevents the plasma from contacting this tube. Additionally, the plasma forms primarily within this gas. To enhance the stability of the plasma, the plasma gas forms a vortex flow [14].

The typical plasma gas in ICPs is argon due to the ease of forming a plasma in this gas. Argon has a low ionization energy. However, Gomes et al. have reported success with an air ICP at atmospheric pressure while Abdallah and Mermet use helium and argon in their ICP device [2, 14].

The innermost tube contains the carrier gas which delivers the sample into the plasma. This tube varies in length depending on the ICP design. Kornblum and de Galen report a recessed probe, while Boulos cites the tube extending even past the length of the intermediate tube [5, 19]. The carrier gas composition also varies in different ICP systems.

For example, the ADA Technologies group uses air as the carrier gas for its sample introduction. Most furnaces and incinerators use air as the working gas or exhaust quench gas. However, to achieve the sensitivity to the metals required by the EPA, the ICPs require the addition of an argon dilution gas to the carrier gas. Because of its low ionization energy, argon forms a plasma more readily than air.

Since the polyatomic species in air store energy in their excited levels, Gomes et al. report lower temperatures in air plasmas than in argon plasmas [14]. Abdallah and Mermet report that a few percent of nitrogen introduced into an argon plasma reduces the plasma temperature [1]. The low temperature in air plasmas impedes the excitation of the sample species and, therefore, depresses the characteristic line radiation emission of the samples. The poor optical signals impede the use of spectroscopic diagnostics [14]. Hence, argon is bled into the carrier gas to promote a high plasma temperature.

The ICP systems also require a laminar sample flow into the ICP. Therefore, a long sampling line is necessary to reduce the velocity of the sample gas from the speed in the duct to a laminar flow regime. A long sample line leads to an inherent loss of the metals on the probe walls.

The sample particles must reside in the plasma for a time long enough to allow for excitation. When these metals de-excite, they emit characteristic line radiation. Measuring the intensity of an element's line emission allows for the determination of the quantity of that element in the exhaust gas. The addition of an argon dilution gas and the reduction of the sample velocity call into question the accuracy of the emission values obtained by ICP systems.

### **1.2.2 Laser Spark**

Physical Sciences, Sandia National Laboratories, and ADA Technologies have developed laser spark devices as continuous emission monitors. The Sandia laser spark monitor uses a Nd:Yag laser to create a tiny plasma in which the hazardous metals become excited. Then a spectrometer collects the atomic emissions of these metals. From this characteristic line radiation, the metals in the exhaust stream are determined.

However, the laser spark systems can only sample a small fraction of the metals in the exhaust duct. This small sampling may not be indicative of the metals in the duct. Additionally, the furnace environment may necessitate a device more robust than the laser [30].

### **1.2.3 Microwave Plasmas**

Microwave-induced plasmas (MIPs) have been used to excite elements for spectroscopic analysis for over two decades. MIPs typically operate at low powers (<500 W) at a microwave frequency of 2.45 GHz. The plasmas are formed in resonant cavity, waveguide, or surface-effect systems [35].

The plasma gas consists of argon, helium, nitrogen, or even air [11, 13, 25, 28, 35].

The injection of liquid aerosols adversely affects the sensitivity of MIPs to trace elements. Forbes et al. report that at atmospheric pressure, the low power of the MIPs can not vaporize nebulized solutions [13]. Okamoto et al. claim that at atmospheric pressure, low power MIPs do not have the necessary energy for atomizing and exciting liquid samples for atomic emission spectroscopy [28]. Therefore, low power MIPs typically are used to study dry gaseous samples [13, 35].

Continuous emission monitors designed to EPA specifications, however, must volatilize and excite the trace hazardous metals which can exist in a liquid matrix or a dry state. Therefore, the Microwave Plasma-Continuous Emissions Monitor (MP-CEM), currently under development at MIT, uses a high-power (1.5 kW) source. Ogura et al. have successfully formed atmospheric pressure nitrogen plasmas at 1 kW, while Ohata et al. have created helium, nitrogen, and air atmospheric pressure plasmas at 1.5 kW [26, 27]. Neither group has reported adverse affects when studying samples dissolved in an aqueous matrix.

The MP-CEM at MIT operates at atmospheric pressure. Most furnace and incinerators use air as their working gas or exhaust quench gas. Ensuring compatibility with these facilities, the MP-CEM also uses air as the working gas. Additionally, the sample line of the MP-CEM consists of a few feet of quartz which minimizes losses of metals to the sampling line walls. The MP-CEM sample probe is modeled after the Method 29 sample probe.

Metal	Transition (nm)	Detection Limit ( $\mu\text{g}/\text{m}^3$ )
As	197.26	144.0
Be	234.86	3.6
Cd	326.12	8.0
Cr	359.35	2.4
Hg	253.65	3.0
Pb	405.78	1.2

Table 1.1: MP-CEM hazardous metals detection limits [34].

The MP-CEM uses a microwave sustained plasma to volatilize and excite the

hazardous metals, and this system uses atomic emission spectroscopy for monitoring trace metals pollution in a stack exhaust. When these metals de-excite, they emit characteristic line radiation. Measuring the intensity of an element's line emission allows for the determination of the quantity of that element in the exhaust gas [12]. This real-time emissions monitor samples the exhaust gas continuously and outputs the metal light signals several times per minute. Table 1.1 shows the current detection limits obtained by the MP-CEM. To meet EPA specifications, the MP-CEM's sensitivity to Hg and As requires improvement.

## **Goal of Research**

Understanding the plasma is essential to increasing the sensitivity of the microwave plasma system to these hazardous metals. Plasma characteristics such as excitation temperature greatly affect the ability of the plasma to excite the hazardous metals. The goal of the research presented in this text is to improve the understanding of the dynamics of an air microwave plasma at atmospheric pressure. The microwave power and gas flow rate regimes determined to maximize the plasma temperature will ultimately be used to develop new detection limits for the hazardous metals.

## **1.3 Outline of Text**

The discussion of the analytical basis for the measurements found in Chapter 2 provides an explanation of the development of spatially resolved electronic excitation temperature profiles. Chapter 3 details the system components of the MP-CEM. The data collection and analysis procedures outlined in Chapter 4, then explain the experimental process of varying the microwave power and the total gas flow rate for this study. Chapter 5 describes, in detail, the characterization of the microwave plasma system through the determination of the effects of varying radius, microwave power, and gas flow rate. Finally, Chapter 6 discusses how the results of this study will help improve the MP-CEM's sensitivity to trace hazardous metals.

# Chapter 2

## Analytical Basis of Measurements

### 2.1 Abel Inversion

The Abel inversion allows for the transformation of line-integrated data to localized values [6]. However, the Abel inversion technique is only valid for cylindrically symmetric geometries [17]. Only variation in the radial direction,  $r$ , is allowed. Additionally, the measured value must fall to zero at the maximum radius,  $R$ . Figure 2.1 shows the geometry of the system.

In the case of the microwave plasma torch (MPT), the Abel inversion technique permits transforming the line-integrated plasma light intensity,  $I(y)$ , into the radial emissivity,  $\varepsilon(r)$ . The line-integrated intensity and the radial emissivity are respec-

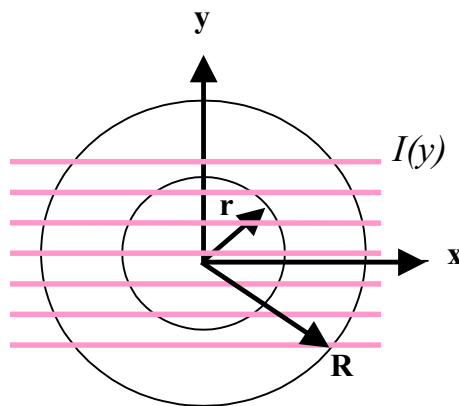


Figure 2.1: Geometry for Abel inversion.



tively given by

$$I(y) = 2 \int_y^R \frac{\varepsilon(r)}{\sqrt{r^2 - y^2}} r dr \quad (2.1)$$

$$\varepsilon(r) = -\frac{1}{\pi} \int_r^R \frac{\frac{dI(y)}{dy}}{\sqrt{y^2 - r^2}} dy \quad (2.2)$$

where  $R$  is the maximum plasma radius [24].  $I(y)$ , the intensity, consists of the energy radiated per wavelength per unit area per unit time within a solid angle,  $(\frac{W}{m^3 sr})$ . The radial emissivity has units of  $\frac{W}{m^4 sr}$ , the energy emitted per wavelength per unit volume per unit time within a solid angle [6].

The plasma light intensity is measured at numerous chordal positions. Section 4.1 details the data collection process. The compilation of the intensity values at all  $y$ -positions gives an experimental  $I(y)$ . Inserting this  $I(y)$  into Equation 2.2 produces the radial value of the emissivity, a local value. This value is used in the calculation of the radial electronic excitation temperature.

## 2.2 Local Thermal Equilibrium

Local thermal equilibrium (LTE) requires that the collisional processes dominate the radiative processes in the plasma [17]. For a plasma in LTE, free electrons and ions form Maxwellian velocity distributions [16]. Additionally, the bound electron population conforms to the Boltzmann distribution [24]. As electrons get excited into different energy levels, equal numbers of electrons de-excite from these energy levels [17]. The populations of electrons in different energy levels are in equilibrium.

LTE varies in only one way from complete thermal equilibrium. In complete thermal equilibrium

$$T_e = T_i = T_{exc} = T_{ion} = T_d = T_{rad} \quad (2.3)$$

where  $T_e$  is the free electron kinetic temperature,  $T_i$  is the ion kinetic temperature,  $T_{exc}$  is the electronic excitation temperature,  $T_{ion}$  is the ionization temperature,  $T_d$  is the dissociation temperature, and  $T_{rad}$  is the blackbody radiation temperature. In

LTE,

$$T_e = T_i = T_{exc} = T_{ion} = T_d \neq T_{rad} \quad (2.4)$$

since all temperatures are equal at LTE except the radiative temperature [6]. Griem maintains that the plasma temperature at LTE describes the distribution function of the species which dominates the reaction rates. In typical plasmas, free electrons dominate the reaction rates [16].

Griem has established a criterion for the determination of a plasma's proximity to LTE. This formulation places a lower limit on the electron density. The Griem criterion states

$$n_e \geq 9 \times 10^{11} \left( \frac{\Delta E}{E_H} \right)^3 \sqrt{\frac{T_e}{E_H}} \quad (2.5)$$

where  $n_e$  is the electron density in  $\text{cm}^{-3}$ ,  $\Delta E$  is the energy level difference between the ground state and the first ionization state,  $E_H$  is the ionization potential for hydrogen, and  $T_e$  is the electron temperature in eV [16]. For argon,  $\Delta E$  has a value of 11.5 eV [22]. The ionization potential of hydrogen,  $E_H$ , is 13.6 eV [20]. Equation 2.5 remains valid only for optically thin plasmas [16]. An optically thin plasma transmits optical wavelengths.

The Griem criterion necessitates the determination of the electron density,  $n_e$ . Timofeev has developed an electron density expression based on experimental data from an atmospheric pressure spherically symmetric microwave air plasma discharge. The electron density is given by

$$n_e = \begin{cases} 5.91 \times 10^{15} e^{-\frac{14.42}{T-1.74}} & (T > 1.74) \\ 0 & (T < 1.74) \end{cases} \quad (2.6)$$

where  $n_e$  is in  $\text{cm}^{-3}$  and  $T$  is the temperature at LTE measured in  $10^3$  K [33]. The MPT system does not have spherical symmetry. However, since microwaves sustain the atmospheric pressure air plasma in the MPT system, this electron density formulation has been adopted.

## 2.3 Electronic Excitation Temperature

For the following calculation of the electronic excitation temperature, the plasma is assumed in LTE. The electronic excitation temperature,  $T_{exc}$ , describes the distribution function of the bound electrons [6]. At LTE, the bound electrons conform to a Boltzmann distribution [24]. As electrons become excited from one energy level,  $E_i$ , to another energy level,  $E_j$ , an equal number of electrons fall from  $E_j$  to  $E_i$  [17]. The population density,  $n$ , of bound electrons in one energy level,  $E_i$ , is given by

$$n_i \propto g_i e^{-\frac{E_i}{T_{exc}}} \quad (2.7)$$

where  $g$  is the statistical weight [17]. The ratio

$$\frac{n_i}{n_j} = \frac{g_i}{g_j} e^{-\frac{E_{ij}}{T_{exc}}} \quad (2.8)$$

compares the population densities of bound electrons in the energy states,  $E_i$  and  $E_j$  [6].  $E_{ij}$  is the energy difference between levels  $E_i$  and  $E_j$ .

To determine  $T_{exc}$ , emission lines from atomic species are used [22]. In the case of the MPT system experiments, introduction of an iron solution into the plasma allows for the examination of this species' atomic emission lines. Section 4.1.2 describes the sample introduction method.

Using the Boltzmann equilibrium, the intensity,  $I_{ij}$ , is given by

$$I_{ij} = \frac{\ell h e^2 N g_j f_{ij} e^{-\frac{E_{ij}}{T_{exc}}}}{2\lambda^3 Q(T) \varepsilon_o m_e} \quad (2.9)$$

where  $\ell$  is the length of the emitting region,  $h$  is Planck's constant,  $e$  is the elementary charge,  $N$  is the total number of atoms of the species of interest,  $f$  is the oscillator strength,  $\lambda$  is the wavelength,  $Q(T)$  is the partition function of the species,  $\varepsilon_o$  is the vacuum permittivity constant, and  $m_e$  is the electron rest mass [3]. Boltzmann equilibrium occurs when equilibrium exists between the neutral ground energy state and the excited atomic energy state [6].

The intensities of the first ionized levels of iron, Fe I, are measured quantities in the MPT system. Each Fe I wavelength has a corresponding energy level, statistical weight, and oscillator strength as seen in Table 2.1 [3]. The calculation of  $T_{exc}$  entails

Wavelength ( $\lambda$ ) (nm)	$E_j$ ( $\text{cm}^{-1}$ )	$\frac{10^{20}\lambda^3}{gf}$ ( $\text{m}^3$ )
368.222	55754	2.6202
368.411	49135	9.5279
370.108	51192	5.1878
370.446	48703	18.8875
371.993	26875	13.8549
372.438	45221	25.8918
372.762	34547	17.1512
373.239	44512	16.4422
373.486	33695	2.5517
373.713	27167	19.3916
374.826	27560	53.8876
374.948	34040	3.5638
375.823	34329	5.3082
376.379	34547	8.258
376.554	52655	1.5757
376.719	34692	11.6964

Table 2.1: Fe I emission lines of interest [3].

plotting the  $\log(I_{ij}\lambda^3/g_i f_{ij})$  versus  $E_j$  [3]. The slope of a straight line fit to these points relates to the electronic excitation temperature by

$$T_{exc} = -\frac{0.625}{m} \quad (2.10)$$

where  $T_{exc}$  is in K, and  $m$  is the slope of the line [6].

## 2.4 Plasma Parameters

Plasma parameters including mean free path and energy collision frequency are important plasma characteristics and essential to understanding the plasma dynamics. The formulations of these parameters follow.

### Electron Velocity

The kinetic energy of the free electrons relates to the electron temperature,  $T_e$ , by

$$v_e = \sqrt{\frac{2 T_e}{m_e}} \quad (2.11)$$

where  $v_e$  is the electron velocity, and  $m_e$  is the rest mass of the electron. Equation 2.11 applies only to nonrelativistic electrons.

### Residence Time

The residence time,  $t$ , describes the amount of time a particle remains in the plasma. The axial and swirl gases constantly flow through the MPT carrying the sample particles in and out of the microwave plasma. The time that the particles reside in the plasma is defined as

$$t = \frac{\ell A}{u} \quad (2.12)$$

where  $\ell$  is the length of the plasma excitation region,  $A$  is the plasma area, and  $u$  is the total gas flow rate. In the MPT system,  $\ell$  is 2 cm.

### Mean Free Path

The mean free path,  $\lambda_{MFP}$ , describes the average distance that a particle travels between collisions. The mean free path of an electron is given by

$$\lambda_{MFP} = \frac{1}{n_g \sigma} \quad (2.13)$$

where  $n_g$  is the neutral gas density, and  $\sigma$  is the cross-section for electron scattering by neutral particles [21]. Timofeev gives  $\sigma$  as  $10^{-15}$  cm<sup>2</sup> for electrons in an atmospheric pressure air microwave plasma [33]. For air at atmospheric pressure,  $n_g$  is given by the ideal gas law

$$n_g = \frac{p}{RT} \quad (2.14)$$

where  $p$  is the pressure,  $R$  is the molar gas constant (8.314 J/K/mol), and  $T$  is the gas temperature [23]. For the MPT,  $p$  equals 1 atmosphere.

### Energy Collision Time and Frequency

Electrons experience a mean time between collisions. The collision time for electrons is defined as

$$\tau = \frac{\lambda_{MFP}}{v_e} \quad (2.15)$$

where  $\tau$  is the energy collision time, and  $v_e$  is given by Equation 2.11 [21]. The energy collision frequency,  $\nu$ , for electrons then relates to the energy collision time by

$$\nu = \frac{1}{\tau} \quad (2.16)$$

where  $\nu$  is typically measured in collisions per second or Hz [21]. The energy collision frequency refers to the frequency that a particle experiences a collision which results in a change in its energy.

### Momentum Collision Frequency

The momentum collision frequency,  $\nu_m$ , relates to the energy collision frequency by

$$\nu_m = \nu \frac{m_1 + m_2}{2m_1} \quad (2.17)$$

where  $m_1$  is the mass of the incident particle, and  $m_2$  is the mass of the target particle [18]. In the case of the MPT system,  $m_1$  is the electron rest mass, and  $m_2$  is the mass of the air molecule. Nitrogen, N<sub>2</sub>, constitutes nearly 80 % of air. Therefore,

the mass of  $N_2$ , 28.02 amu, is used for  $m_2$  [23]. The momentum collision frequency refers to the frequency that a particle, in this case an electron, experiences a collision which results in a change in its momentum.

### Electron Plasma Frequency

The electron plasma frequency,  $\omega_{pe}$ , is given by

$$\omega_{pe} = \left( \frac{n_e e^2}{\epsilon_o m_e} \right)^{\frac{1}{2}} \quad (2.18)$$

where  $n_e$  is the electron density calculated from Equation 2.6,  $e$  is the elementary charge,  $\epsilon_o$  is the vacuum permittivity constant, and  $m_e$  is the rest mass of the electron [24].

### Skin Depth

Lieberman and Lichtenberg describe the collisional skin depth,  $\delta$ , by

$$\delta = \frac{\sqrt{2} c}{\omega_{pe}} \left( \frac{\nu_m}{\omega} \right)^{\frac{1}{2}} \quad (2.19)$$

where  $c$  is the speed of light in a vacuum,  $\omega_{pe}$  is the electron plasma frequency from Equation 2.18,  $\nu_m$  is the momentum collision frequency from Equation 2.17, and  $\omega$  is the microwave frequency [21]. Section 5.4 discusses the determination of the collisional skin depth of the microwave wavelength in the MPT. The microwave frequency of the system is 2.45 GHz which corresponds to  $\omega$ . Equation 2.19 remains valid only if  $\omega_{pe}, \nu_m \gg \omega$  [21].

### Plasma Conductivity

The plasma conductivity,  $\sigma_{dc}$ , is given by

$$\sigma_{dc} = \frac{2}{\omega \mu_o \delta^2} \quad (2.20)$$

where  $\omega$  is the microwave frequency,  $\mu_o$  is the vacuum permeability constant, and  $\delta$  is the collisional skin depth given by Equation 2.19 [21]. The microwave frequency of the system is 2.45 GHz. Equation 2.20 remains valid only if  $\omega_{pe}, \nu_m \gg \omega$  [21].

## 2.5 Microwave Parameters

The characteristics of the microwave greatly impact the plasma. The cutoff frequency of the microwaves and the wavelength propagating in the waveguide provide essential information.

### Cutoff Frequency

In a vacuum, the wavelength,  $\lambda$ , relates to the frequency,  $\omega$ , by

$$\lambda = \frac{c}{\omega} \quad (2.21)$$

where  $c$  is the speed of light in a vacuum [8]. The cutoff frequency corresponds to the longest wavelength that will propagate in the waveguide. This frequency depends on the geometry of the waveguide in which the microwaves propagate. The cutoff frequency in a rectangular waveguide is given by

$$\omega_c = \frac{c}{2a} \quad (2.22)$$

where  $a$  is the widest dimension of the waveguide cross section [32]. The width of the WR-284 waveguide used in these experiments is 7.21 cm.

### Propagating Wavelength

Equation 2.21 gives the wavelength in free space. However, since the microwaves propagate in the confined region of the waveguide, the wavelength of the microwaves



traveling in the waveguide,  $\lambda_g$ , is given by

$$\lambda_g = \frac{\lambda}{\left[1 - \left(\frac{\omega_c}{\omega}\right)^2\right]^{\frac{1}{2}}} \quad (2.23)$$

where Equation 2.21 yields  $\lambda$ , Equation 2.22 gives  $\omega_c$ , and  $\omega$  is the microwave frequency of the magnetron [32]. The microwave frequency,  $\omega$ , is 2.45 GHz.

# Chapter 3

## Apparatus

The MP-CEM consists of four main systems: the microwave plasma torch (MPT) system, the gas flow system, the sample injection system, and the optics system.

### 3.1 Microwave Plasma Torch System

The MPT system entails the power supply, magnetron, and waveguide (see Figure 3.1). The ASTEX power supply and magnetron have the capacity for 1.5 kW of microwave output power at 2.45 GHz. A conventional microwave oven typically operates between 600 W and 800 W at 2.45 GHz. Using this frequency of microwaves keeps the cost of the MPT system low, since magnetrons that produce 2.45 GHz are manufactured en masse for consumer products.

During the experiments, the MPT runs between 0.9 kW and 1.4 kW forward power. A circulator with a water-cooled load prevents reflected power from damaging the magnetron. Also, a waveguide section equipped with tuning stubs allows the user to match the impedance manually to decrease the amount of reflected power. Typically, the MPT system runs with less than one percent of the forward power reflected.

The tuning stub section of the waveguide continues into the shorted brass WR-284 waveguide (see Figure 3.1). A 3.5 cm diameter cavity is located a quarter of a wavelength, 5.7 cm, from the shorted end of the waveguide. A hollow quartz

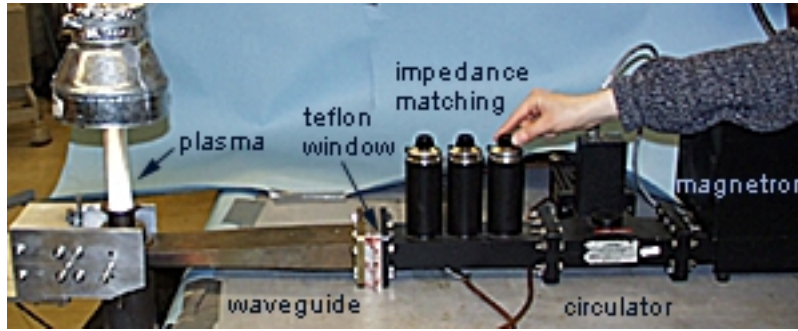


Figure 3.1: Microwave plasma torch system.

cylinder sits inside the cavity. In previous experiments, a boron nitrite (BN) cylinder has resided in the cavity [15]. Quartz and BN are both dielectric materials nearly transparent to the 2.45 GHz microwave frequency. However, for all of the experiments discussed here, the hollow cylinder must also be transparent to visible and ultraviolet wavelengths. BN prevents the transmission of ultraviolet and visible wavelengths. Quartz does transmit all of these wavelengths which facilitates the study of the atomic emissions in the plasma. Therefore, a quartz cylinder is used to contain the plasma in these experiments.

To keep the circulator and magnetron clean, a teflon window is located in the connection between the brass waveguide section and the tuning stub section. The teflon window allows the transmission of the 2.45 GHz microwave frequency. Occasionally, the plasma forms in the waveguide or on the surface of the teflon window due to deposits. In the unlikely event that the containment fails, the plasma fireball must burn through this teflon window to travel further up the waveguide. The change in operating parameters alerts the operator to turn off the power supply thereby killing the plasma. Thus, the teflon window functions only as protection for the magnetron. If the plasma extends past the teflon window, the plasma can severely damage the magnetron.

Another cause of a plasma forming in the waveguide involves debris inside the waveguide. Any rough surface provides a spot for a plasma to form. In fact, starting the plasma involves inserting a metal wire into the hollow quartz cylinder. At a quar-

ter of a wavelength from the shorted end of the waveguide, the electric field, E-field, reaches its maximum value. To breakdown air at atmospheric pressure requires an E-field of  $\sim 1.5$  kV/cm. Even at its maximum value, the E-field in the MPT does not reach this value. Inserting a tungsten, W, wire into the waveguide, however, concentrates the E-field enough to breakdown the air (see Appendix A). The microwave power then completely sustains the plasma.

## 3.2 Gas Flow System

The gas flow system helps maintain the containment of the plasma. This system consists of an axial gas feed and a swirl gas feed (see Figure 3.2). For all of the experiments, the swirl and axial gas flows originate from the in-house compressed air feed. In prior experiments, the swirl and axial gases have consisted of pure nitrogen or a combination of nitrogen and compressed air [15]. The sole use of compressed air in these experiments stems from a desire to simulate actual in situ conditions as closely as possible. Air operates as the working gas and as the exhaust quench gas in many furnace and incinerator environments. Thus, air is chosen as the working gas in the MP-CEM.

The axial flow provides the air for ionization when igniting and running the plasma. After starting the plasma, the swirl gas continually sweeps around the inner surface of the hollow quartz cylinder. The swirl gas enters into a hollow ring in the base of the bronze can. Three jets exit the ring slightly below the quartz cylinder. The jets are equally spaced around the can and are angled slightly up towards the quartz cylinder. The swirl gas enters the bottom of the quartz cylinder and sweeps around its sides. The plasma must not remain in contact with the quartz surface, since quartz melts at  $\sim 800^\circ\text{C}$ . The plasma temperature, however, greatly exceeds the quartz melting point (see Section 5.2). The sweeping motion of the swirl gas confines the plasma and prevents the attachment of the plasma to the quartz cylinder walls.

Sometimes, debris or water clogs one or more of the jets adversely affecting the confinement of the plasma. Unfortunately, the jets are brazed into the can preventing

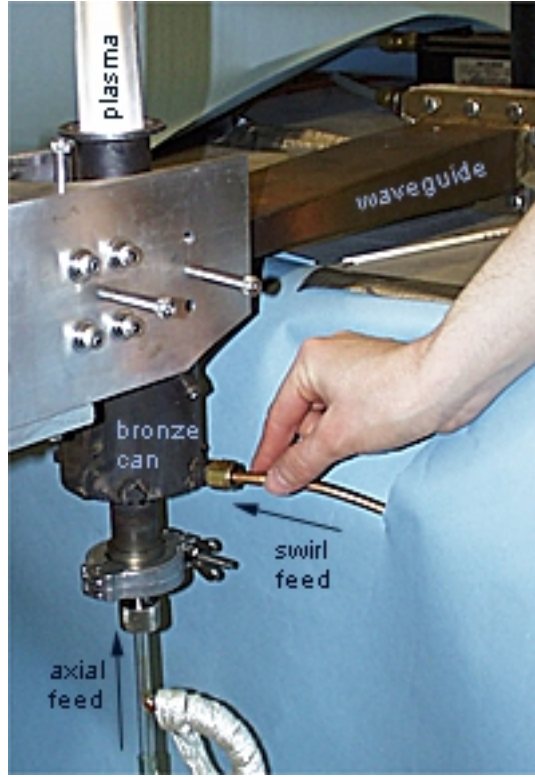


Figure 3.2: Gas flow system.

their removal for cleaning. Blasting high pressure air through the swirl gas line will clear the jets. The axial gas tube, the hollow quartz cylinder, water, and debris should be removed before cleaning the jets.

Pollack documents the necessity of maintaining constant axial and swirl gas flow rates [31]. Therefore, both the axial and swirl flows are closely monitored in all experiments. To ensure constant gas flow rates, pressure regulators, needle valves, and pressure gauges have been mounted on the axial and swirl air lines. Also, calibrated OMEGA industrial rotameters measure the axial and swirl gas flow rates. The following equation converts the Omega readings to standard units

$$u = \sqrt{\frac{\rho \times (T + 460)}{36 \times p}} \times \frac{v \times s}{100} \quad (3.1)$$

where  $u$  is the gas flow rate at standard temperature and pressure (STP) in units of cubic feet per minute (cfm),  $\rho$  is the specific gravity of the gas at 70°F and STP,  $T$

is the temperature of the gas in °F,  $p$  is the pressure of the gas in pounds per square inch (psi),  $v$  is the flow rate measured by the Omega meter, and  $s$  is the scale factor of the particular flowmeter [29]. In the case of air,  $\rho$  equals 1,  $T$  equals 70°F, and  $p$  equals the value measured by the pressure gauge plus 14.7 psi. The scale factors for the axial and swirl gas rotameters are 0.00865 and 0.00849 respectively.

Even with these regulators the gas flow rate readings may fluctuate, especially during the initial run time. During the first thirty minutes of operation, the waveguide and the bronze can rise to an equilibrium temperature. Therefore, the plasma must run for at least thirty minutes to allow the waveguide temperature to equilibrate before beginning an experiment.

### 3.3 Sample Injection System

In addition to feeding the plasma, the axial gas also transports the particulates from the sample injection system into the plasma. The sample injection system primarily consists of the nebulizer, the spray chamber, the waste container, and the quartz y-tube (see Figure 3.3). The Meinhard nebulizer consists of two concentric tubes. The inner capillary tube carries the acid solution which contains the dissolved metals of interest. A continuous flow of nitrogen gas at 40 psi fills the outer tube. As the Cole-Parmer peristaltic pump sends the liquid into the nebulizer, the nebulizer aerosolizes the solution and ejects the mist into the spray chamber. The spray chamber limits the size of the droplets which enter the axial gas stream. All of the large particles enter the waste container. In fact, over 99 % of the original metal solution discharges into the waste container [12].

The exhaust gas of a furnace which exits into the environment has already travelled through scrubbers and particulate filters. Therefore, the particulates ejected by these facilities have small diameters. The spray chamber is used in the MP-CEM to limit additional water loading. The tiny droplets travel from the spray chamber into the quartz y-tube. The heater tape wrapped around the y-tube converts the droplets to dry particulates. The axial gas enters one branch of the y-tube and the spray chamber

connects to the other branch (see Figure 3.3). At the junction of the two branches, the axial gas picks up the particulates and transports them into the plasma.

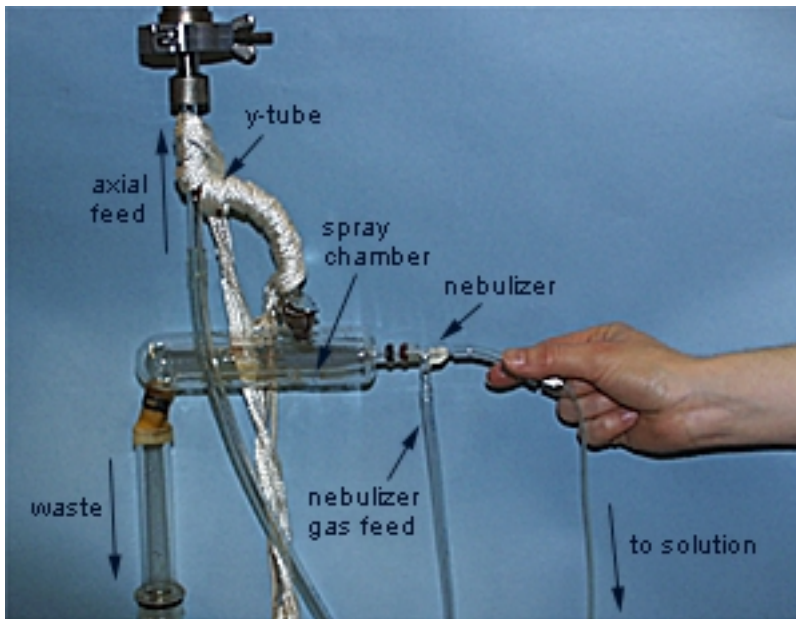


Figure 3.3: Sample injection system.

### 3.4 Fiber Optics System

The plasma disassociates molecular species, and then electron-atom collisions lead to the excitation of the hazardous metal particulates once inside the plasma. When the metals undergo de-excitation or recombination, they emit characteristic line radiation. The fiber optics system measures these photons. The optics system consists of a series of lenses, a translation stage, a fiber optic, a spectrometer, and a data acquisition system (see Figure 3.4). A 3.175 cm by 1.27 cm hole in the shorted end of the brass waveguide facilitates the study of the atomic emissions. The small size of the hole prevents leakage of microwave radiation. The microwave frequency is cutoff.

A series of two lenses then magnifies the plasma light by a factor of two and projects the image into a focal plane. The fiber optic sits in this focal plane. The fiber optic attached to a translation stage can scan the entire diameter of the plasma. Section 4.1.2 discusses the acquisition of the plasma light. The fiber optic system has

a 2 mm resolution. The translation stage allows measurements as close together as 1 mm.

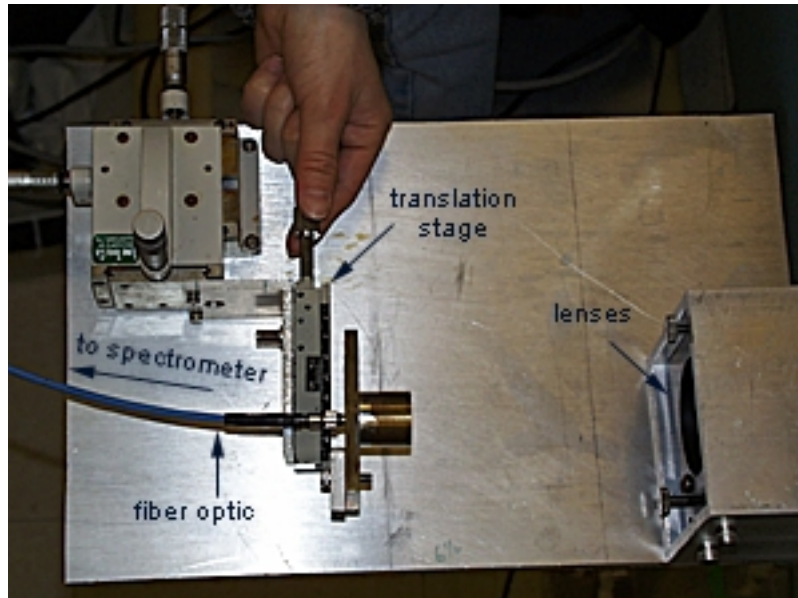


Figure 3.4: Optics system.

The fiber optic leads to an Instruments S.A. Model THR-640 spectrometer which has a 2400 groove/mm grating, an adjustable slit, and a Princeton Instruments Model IRY-512W intensified 512-element detector array. The spectral resolution is about 0.05 nm with an instantaneous spectral range of about 6.5 nm that can be tuned from 180 nm to 600 nm. The spectrometer attaches to a computer with a Pentium processor. The data acquisition software is CSMA from Princeton Instruments. In the visible to ultraviolet regime, the spectrometer's sensitivity varies greatly. However, since the instantaneous spectral range is only 6.5 nm, the grating efficiency is assumed to be relatively constant. The CSMA software does allow for a background subtraction which corrects for some of the variance in the spectrometer's sensitivity in the 6.5 nm window. Section 4.1 discusses the pertinent abilities of the CSMA software package.



# Chapter 4

## Data Collection and Analysis

### Procedures

For all experiments, the data are collected and analyzed in a systematic manner. The data collection procedures envelop the air flow settings to the physical scanning of the plasma. The data analysis methodology includes the conversion of raw data to the electronic excitation temperature calculation.

#### 4.1 Data Collection

For every experiment, physical parameters such as the gas flow rate and the input microwave power must be determined. Throughout the experiment, these parameters are monitored and recorded to aid in the data analysis. Additionally, data collection procedures are followed to limit the introduction of error into the final electronic excitation temperature measurements.

##### 4.1.1 Apparatus Settings

###### Gas Flow Rate and Nebulizer

Appendix B outlines the procedure for starting the MPT, controlling the input microwave power, and setting the axial and swirl gas flow rates. The nebulizer requires

40 psi of nitrogen gas in its gas feed line to operate properly. Additionally, the 3 o'clock speed setting allows the Cole-Parmer peristaltic pump to supply the nebulizer with a proper rate of solution,  $\sim 1$  mL/min, during all experiments.

## Spectrometer

As described in Section 3.4, the spectrometer has an instantaneous spectral range of  $\sim 6.5$  nm. Tuning the spectrometer to the proper region is essential to collecting the intensity data of the lines of interest. The wavelength in nm of the central pixel roughly corresponds to one half the spectrometer reading since a grating with twice the dispersion compared to the original spectrometer design is used. For these experiments, the spectrometer reads  $\sim 749.95$ . The iron lines of interest fall in the range between 368 nm to 376 nm (see Table 2.1). The spectrometer is set to observe wavelengths between 370 nm and 377 nm. Additionally, adjusting the spectrometer slit optimizes the line intensity to line width ratio.

## CSMA

The data acquisition software, CSMA, integrates the plasma light intensity measurements for a certain amount of time referred to as the exposure time. The exposure time for all discussed experiments is set to 0.5 seconds. A single snapshot, called a frame, of the spectrum consists of 512 pixels or channels. Each channel corresponds to a particular wavelength (see Section 4.2.1). The number of frames collected is also controlled within CSMA. Each frame consists of the plasma light intensity measured within each of the 512 channels during the exposure time. In these experiments a data set consists of 25 frames.

CSMA is capable of removing the background noise associated with the spectrometer. Acquiring only the background associated with the spectrometer, or the dark noise, requires covering the fiber optic with an opaque cloth while instructing CSMA to collect the background spectrum. CSMA integrates the dark noise for each pixel during the exposure time. Then, CSMA automatically subtracts this background value from each pixel during data collection. The background subtraction technique

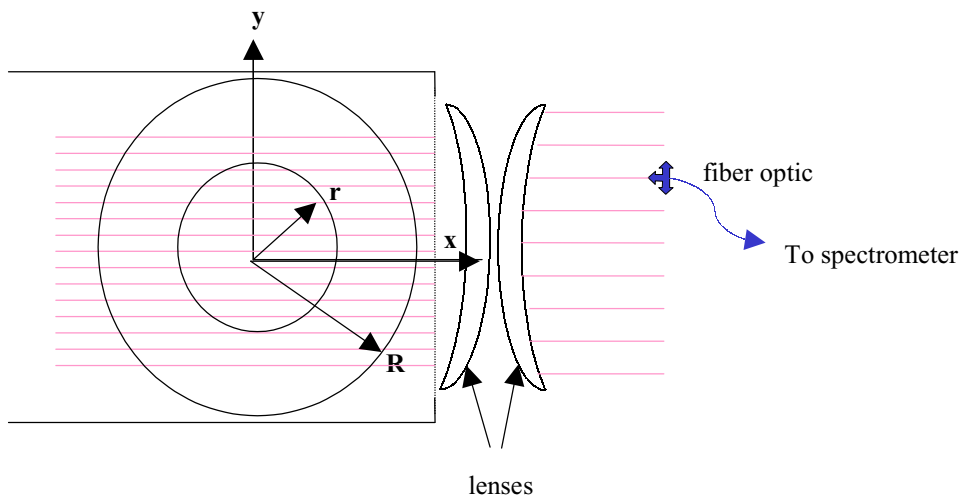


Figure 4.1: Schematic of scanning the plasma.

is used for all experiments.

### 4.1.2 Scanning the Plasma

As described in Chapter 3, a series of lenses magnify and project the plasma light onto the plane in which the fiber optic sits. The fiber optic located on a translation stage scans the full diameter of the projection of the plasma. Data collection occurs for up to sixty-six chords evenly spaced in one millimeter increments (see Figure 4.1).

#### Measurements at Each Chord

At each chord position, two sets of data are acquired. The first set requires using the nebulizer to inject iron dissolved in a nitric acid matrix into the plasma. The Alpha Aesar calibrated solution consists of 10,000  $\mu\text{g}/\text{mL}$  of iron dissolved in 5 % nitric acid. While the aerosolized particles from the iron solution traverse the plasma, the data acquisition system collects twenty-five frames of the iron spectrum in the 370 nm to 377 nm range. Each snapshot contains light integrated for 0.5 seconds as described in Section 4.1.1.

The second data set requires injecting deionized (DI) water into the plasma to obtain a blank water background. The data acquisition system collects twenty-five

frames of this background spectrum. The DI water runs through the nebulizer for at least 30 seconds before data are collected. Preventing contamination of the water signal by the iron is essential to data analysis.

## **Reference Chords**

During the course of the experiment, iron oxide gradually coats the interior of the hollow quartz cylinder containing the plasma. This deposition, of course, affects the light intensity collected by the optics system. To determine the optical degradation of the quartz, the water background and iron files for a particular reference chord are periodically repeated to follow this degradation. The reference chord data are collected at the beginning of the experiment, at the end of the experiment, and after every fifth chord during the experiment. The reference chord for all of these experiments is position 25. This chord is located  $\sim 6$  mm from the center chord. Therefore, the light intensity collected remains strong even after significant coating. The analysis of the quartz degradation is given in Section 4.2.2.

## **4.2 Data Analysis**

Developing the radial profile of the electronic excitation temperature in the MPT requires several processing steps. The procedure follows.

### **4.2.1 Conversion of Data**

After completing the scan of the plasma, each pixel is averaged over the twenty-five frames in the data set for each chord position using the Spyglass Macro depicted in Appendix C. A data set consists of a CSMA file containing 25 frames. Each data set possesses the spectra of either a water background or the iron solution at a particular chord position. Next, for a given chord, the water background value for each pixel is subtracted from its respective pixel in the iron spectrum using the Excel Macro shown in Appendix D.

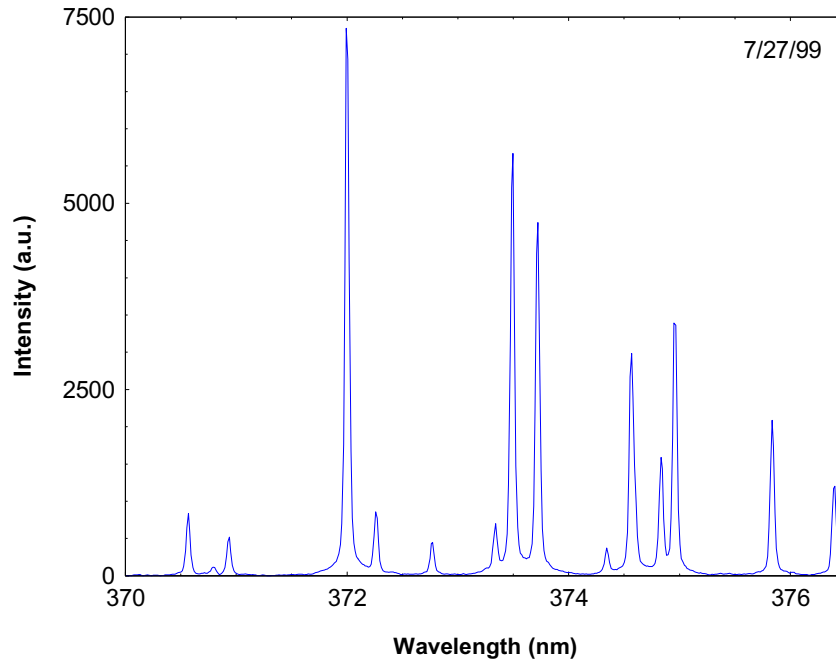


Figure 4.2: Typical atomic iron (Fe I) spectrum.

The iron solution consists only of water, iron, and nitric acid. Subtracting the water background from the iron spectrum removes the influence of the water loading on the plasma light intensity. All remaining signal light is assumed due only to the influence of the iron in the plasma. The influence of the nitric acid on the plasma is assumed negligible. The removal of the influence of the water loading leaves an iron spectrum as shown in Figure 4.2 for a particular chord.

Using the CRC wavelength tables, the wavelengths of the iron lines are determined. Having obtained a calibrated spectrum, the pixel numbers for the iron lines of interest are run through the Excel Macro shown in Appendix E. This program outputs each iron line of interest and its intensity value at each chord position.

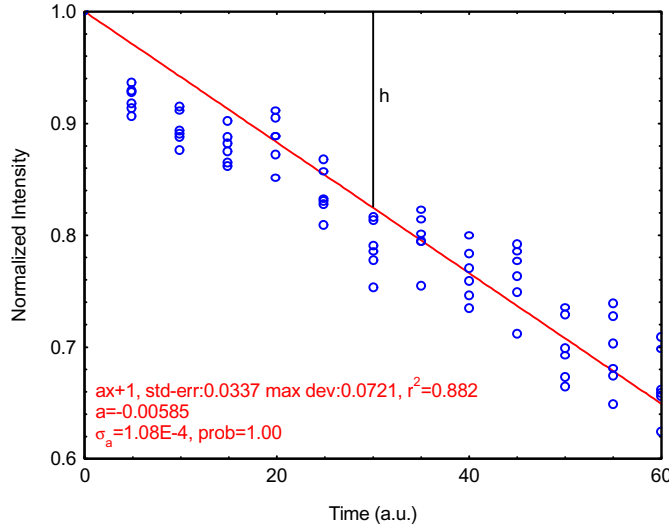


Figure 4.3: Degradation curve of quartz cylinder.

## 4.2.2 Intensity Measurements

### Quartz Degradation Correction

Section 4.1.2 describes the gradual degradation of the quartz cylinder during an experiment. To quantify this degradation, the intensities of several strong Fe I lines are examined. The intensity values of each line are normalized to the initial intensity value for that line.

The degradation of the quartz occurs during the length of the experiment. The reference chord data are collected at the beginning of the experiment, at the end of the experiment, and after every 5 chord position acquisitions. Thus, time,  $t=0$ , corresponds to the reference chord data collected at the beginning of the experiment. Time,  $t=5$ , corresponds to the reference chord data collected after water background and iron solution data sets have been acquired at chord positions 0 through 5. The reference chord position for these experiments is 25.

The normalized intensity values for all of the Fe I lines are plotted against time as shown in Figure 4.3. If the quartz experiences no degradation, all intensity values for the reference chord will remain constant over time. Figure 4.3 reveals that degradation of the quartz does, indeed, occur. Assuming a linear degradation, a line is fit through

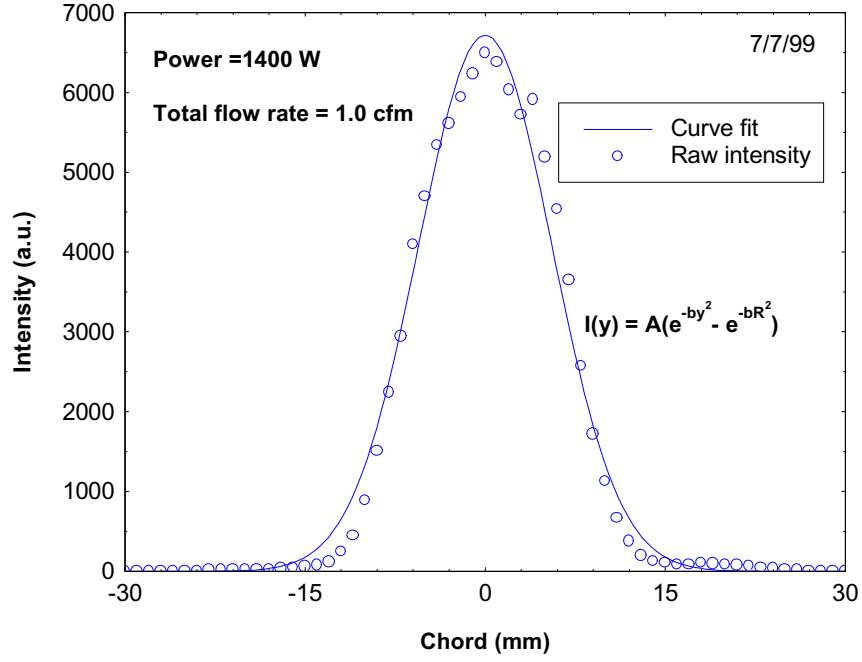


Figure 4.4: Typical intensity profile.

these points. The fractional vertical offset,  $h$ , at each time is given by

$$h = t\sqrt{1 + a^2} \sin \left( \cos^{-1} \left( \frac{1}{\sqrt{1 + a^2}} \right) \right) \quad (4.1)$$

where  $t$  is the time, and  $a$  is the slope of the line. The corrected intensity,  $I_t$ , at any time is given by

$$I_t = hI_o + i_t \quad (4.2)$$

where  $I_o$  is the intensity of the line at time  $t = 0$ , and  $i_t$  is the measured intensity of the line at time  $t$ .

### Intensity Profile

Having used Equation 4.2 to correct for the quartz degradation, the intensity data for each iron line is plotted versus chord position. Figure 4.4 shows a typical intensity profile.

To apply the Abel inversion technique as described in Section 2.1 requires a sym-

metric intensity function as well as the necessity for the intensity to fall to zero at the plasma edge. To ensure that these specifications are met, a subtracted Gaussian is fit to the intensity profile data of each iron line (see Figure 4.4). This curve has the form

$$I(y) = Ae^{-by^2} - Ae^{-bR^2} \quad (4.3)$$

where  $I(y)$  is the intensity fitted to the raw data,  $R$  is the maximum radius, and  $A$  and  $b$  are fitting parameters unique to each intensity profile.

### 4.2.3 Emissivity Profiles

The Abel technique transforms line-integrated data,  $I(y)$ , into localized values, the radial emissivity,  $\varepsilon(r)$  (see Section 2.1). The Gaussian fitted intensity profile, Equation 4.3, is inserted into the Abel emissivity formula, Equation 2.2. Since this integration is solvable analytically, each iron line is Abel inverted to obtain the derived radially localized emissivity

$$\varepsilon(r) = \frac{1}{\sqrt{\pi}} Ab^{\frac{1}{2}} e^{-br^2} \text{erf}([b(R^2 - r^2)]^{\frac{1}{2}}) \quad (4.4)$$

where  $r$  is the radial parameter, and  $A$  and  $b$  are fitting parameters unique to each Fe I line intensity profile as defined in Equation 4.3. Appendix F explains the details of this calculation. Figure 4.5 shows the emissivity profile for a typical iron line.

### Validity of Abel Inversion Calculation

Before using the emissivity to determine the electronic excitation temperature as described in Section 2.3, the validity of the Abel inversion is verified. The derived emissivity, Equation 4.4, is plugged into the Abel intensity formulation, Equation 2.1. The output should yield Equation 4.3, the Gaussian fitted to the intensity data. This manipulation, shown in Appendix F, yields the reconstructed intensity which is given by

$$I(y)_{rec} = \frac{2}{\sqrt{\pi}} Ae^{-by^2} \int_0^{\sqrt{b(R^2 - y^2)}} e^{-x^2} \text{erf}([b(R^2 - y^2) - x^2]^{\frac{1}{2}}) dx \quad (4.5)$$



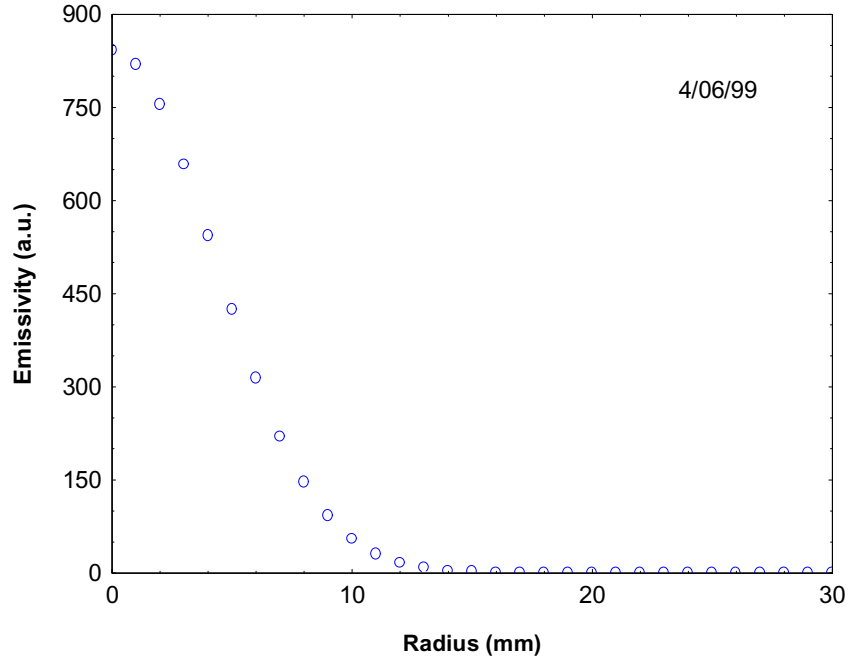


Figure 4.5: Typical emissivity profile.

where  $y$  is the chord position. This equation clearly has no analytical solution. Therefore,  $I(y)_{rec}$  is solved numerically using the Excel Macro in Appendix G. For comparison, the reconstructed intensity, Equation 4.5, and the original intensity, Equation 4.3, are plotted in Figure 4.6. The two curves coincide almost exactly. Therefore, the Abel inversion is proved valid for these calculations.

#### 4.2.4 Electronic Excitation Temperature

Assuming LTE as discussed in Section 2.2, a comparison of the relative emissivity values of different iron lines at a single radial point will yield the electronic excitation temperature,  $T_{exc}$ , of the plasma. As described in Section 2.3, each Fe line has an associated energy level,  $E$ , oscillator strength,  $f$ , and statistical weight,  $g$  (see Table 2.1).

At a single radius, plotting  $\log(\varepsilon(r)\lambda^3/gf)$  versus  $E$  for each iron line yields a graph such as Figure 4.7. A straight line fit through these points creates a slope inversely

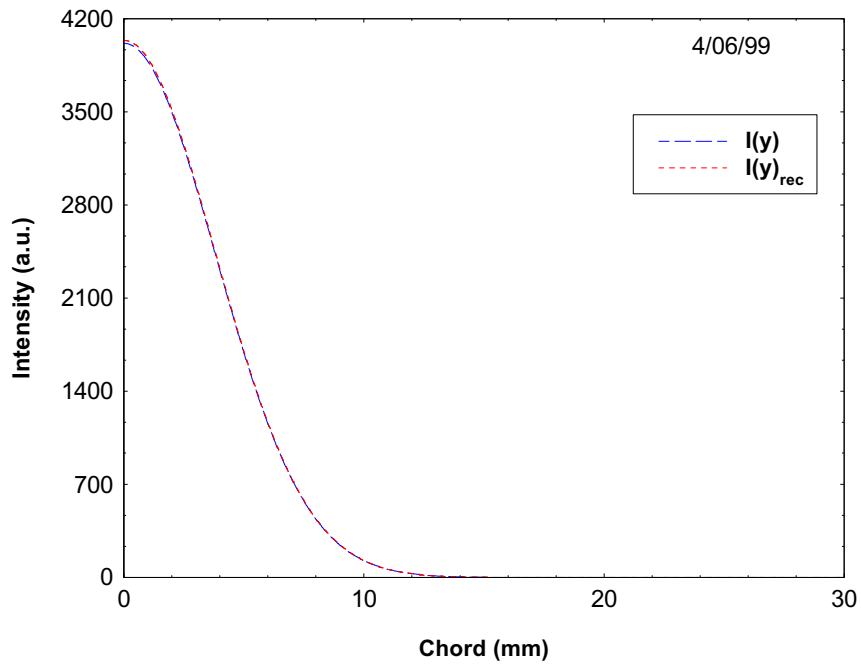


Figure 4.6: Comparison of numerically reconstructed intensity,  $I(y)_{rec}$ , and original intensity,  $I(y)$ .

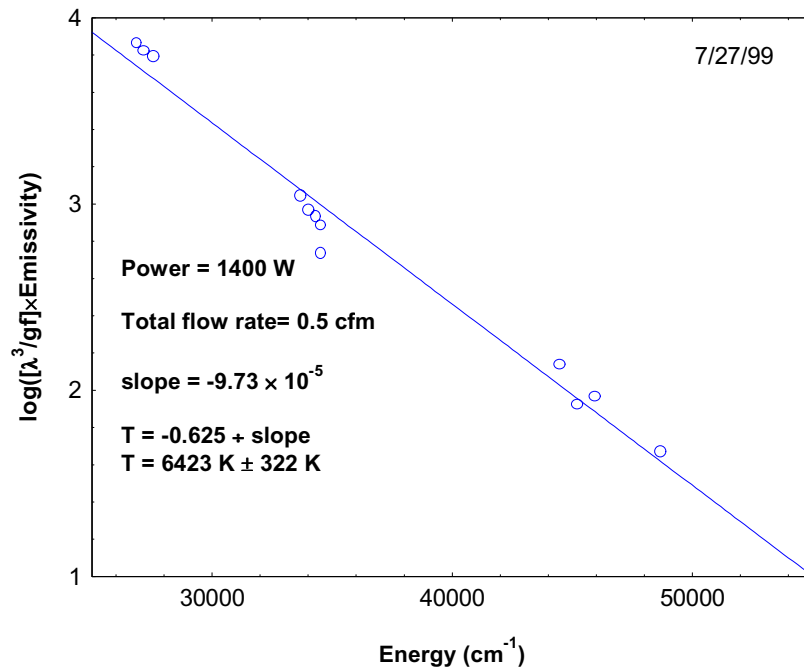


Figure 4.7: Determination of electronic excitation temperature.

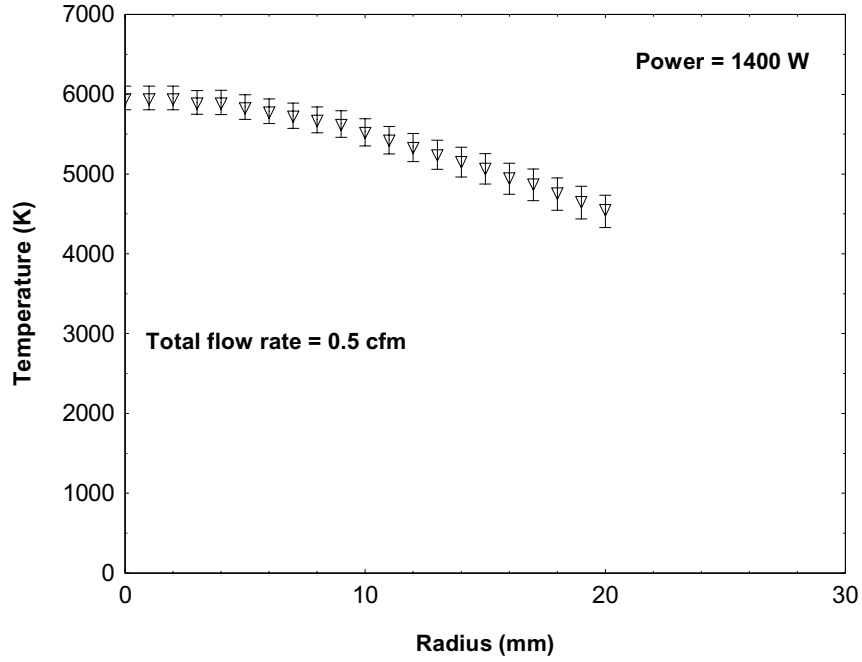


Figure 4.8: Electronic excitation temperature profile.

proportional to  $T_{exc}$  (see Section 2.3). Using Equation 2.10 reveals an electronic excitation temperature,  $T_{exc} = 6423 K \pm 322 K$ , in Figure 4.7. The deviation from the straight line determines the error in  $T_{exc}$ . The standard deviation of the points fit to the line divided by the slope of the line yields the fractional error in  $T_{exc}$ .

Performing this calculation at each radial point provides the  $T_{exc}$  profile in the plasma (see Figure 4.8). Since the emissivity values decline rapidly near  $r = 20$  mm, the error in  $T_{exc}$  becomes quite large beyond this range. Therefore, the  $T_{exc}$  profile measurements extend only to this region.

Figures 4.9 and 4.10 summarize the data collection and analysis procedures used for the determination of the emissivity and electronic excitation temperature profiles.

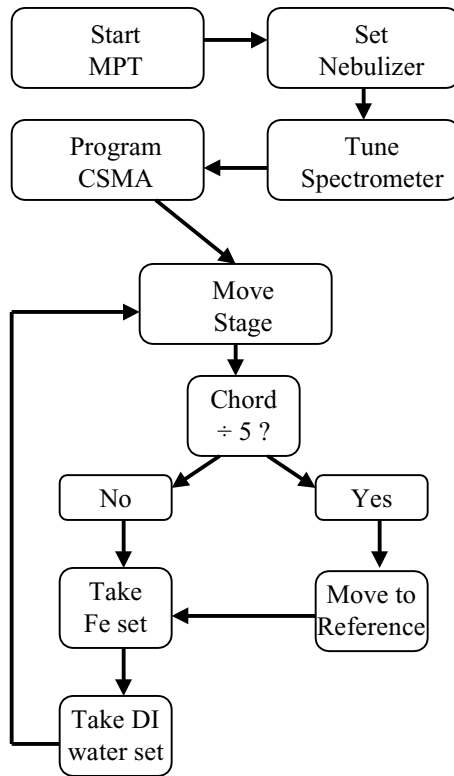


Figure 4.9: Flow chart of data collection procedure.

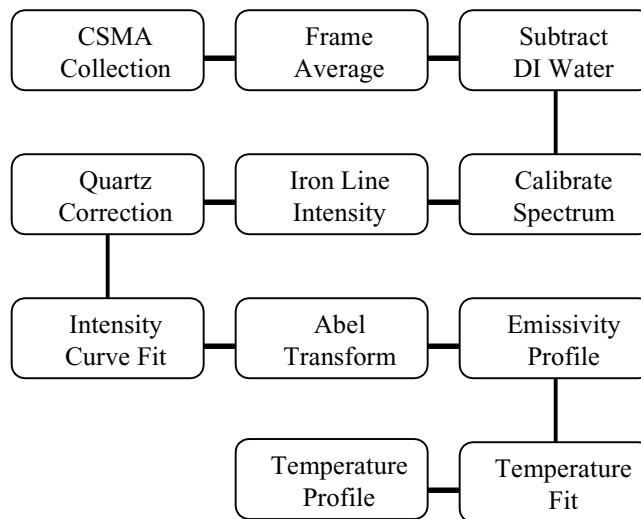


Figure 4.10: Flow chart of data analysis procedure.

# Chapter 5

## Results and Discussion

The input microwave power and the total gas flow rate affect the emissivity and the electronic excitation temperature profile measurements. To quantify these effects, a series of experiments have been performed. In these tests, one parameter remains constant while varying the other factor. The radial variation of the emissivity and the electronic excitation temperature have been studied in different microwave power and gas flow rate regimes.

### 5.1 Emissivity Profiles

The emissivity profiles yield the effects of microwave power and total gas flow rate on the diameter of the plasma. Normalizing the emissivity profile values to the on-axis emissivity value emphasizes these variations. Therefore, the emissivity values have been normalized in these profile studies.

#### 5.1.1 Microwave Power Variation

Throughout the microwave power experiments, the total gas flow rate remains constant at 0.5 cfm. Using the data collection procedures outlined in Section 4.1, the data are collected at three microwave power levels, 900 W, 1150 W, and 1400 W. As stated in Section 3.1, the reflected power typically consists of less than 1 % of

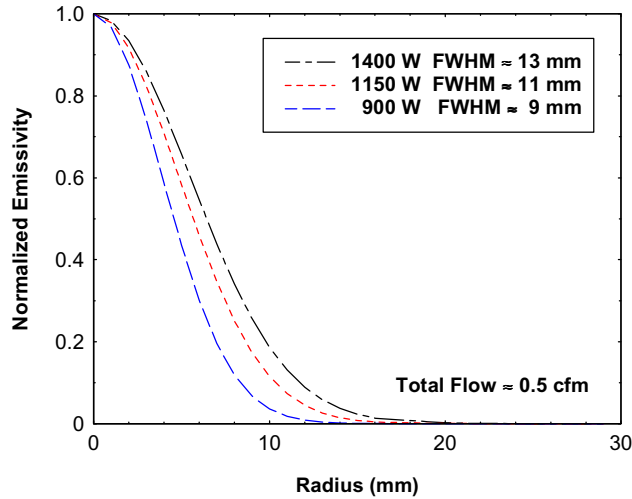


Figure 5.1: Normalized emissivity at constant flow rate with varying power for a representative Fe I transition.

the forward power. In each of these cases, the reflected power remains within this parameter.

For each power level, a complete scan of the diameter of the plasma is performed as described in Section 4.1.2. Following the data analysis procedures detailed in Section 4.2, the emissivity profiles are determined at each power level.

Figure 5.1 depicts the normalized emissivity values for a representative Fe I transition for this experiment. The FWHM values characterize the change in the plasma diameter. In Figure 5.1, the diameter of the plasma grows as the power increases. With a 28 % increase in the microwave power from 900 W to 1150 W, the plasma diameter expands by 22 %. Likewise, with a 22 % increase in power from 1150 W to 1400 W, the plasma diameter enlarges by 18 %. Similarly, Abdallah and Mermet report an inflation in their inductively coupled argon plasma with an increase in power [2].

This result demonstrates that increasing the microwave power allows for the breakdown of gases further from the core of the plasma. The addition of microwave power allows the plasma to expand and fill a greater volume of the quartz cylinder. As the microwave power increases by 55 % from 900 W to 1400 W, the volume of the plasma

expands by over 100 %.

Pollack states that the sample entering the plasma experiences diffusion away from the center of the plasma [31]. The expansion of the plasma diameter at high microwave power ensures an enlarged region in which the hazardous metals may experience excitation by the plasma.

### **5.1.2 Gas Flow Rate Variation**

During the gas flow rate variation experiments, the input microwave power remains constant at 1400 W with less than 1 % reflected power. For these tests, the total gas flow rate entails the summing of the axial gas flow rate and the swirl gas flow rate. Section 3.2 gives a description of the gas flow system.

Following the data collection procedures in Section 4.1, four total gas flow rate regimes, 0.4 cfm, 0.5 cfm, 0.8 cfm and 1.0 cfm, are examined. For the 0.5 cfm case, the axial gas flow rate constitutes 0.3 cfm of the total gas flow rate while the swirl gas flow rate makes up 0.2 cfm. In all of the other gas flow rate regimes, the axial and swirl gas flow rates constitute equal portions of the total gas flow rate. For each total flow rate regime, the entire diameter of the plasma is scanned, and the data are analyzed to produce emissivity profiles.

Figure 5.2 displays the results of this study. The FWHM values, indicative of the plasma diameter, decrease as the total gas flow rate increases. This result indicates an improved confinement of the plasma by increasing the total gas flow rate. In fact, the plasma volume decreases by over 25 % when the gas flow rate is increased from 0.4 cfm to 1.0 cfm. This result is particularly relevant to interpreting the electronic excitation temperature results discussed in Section 5.2.2. Therefore, Section 5.2.2 details the effect of the total gas flow rate on the volume of the plasma.

## **5.2 Electronic Excitation Temperature Profiles**

The electronic excitation temperature is determined at each radial point using the method outlined in Section 4.2.4.

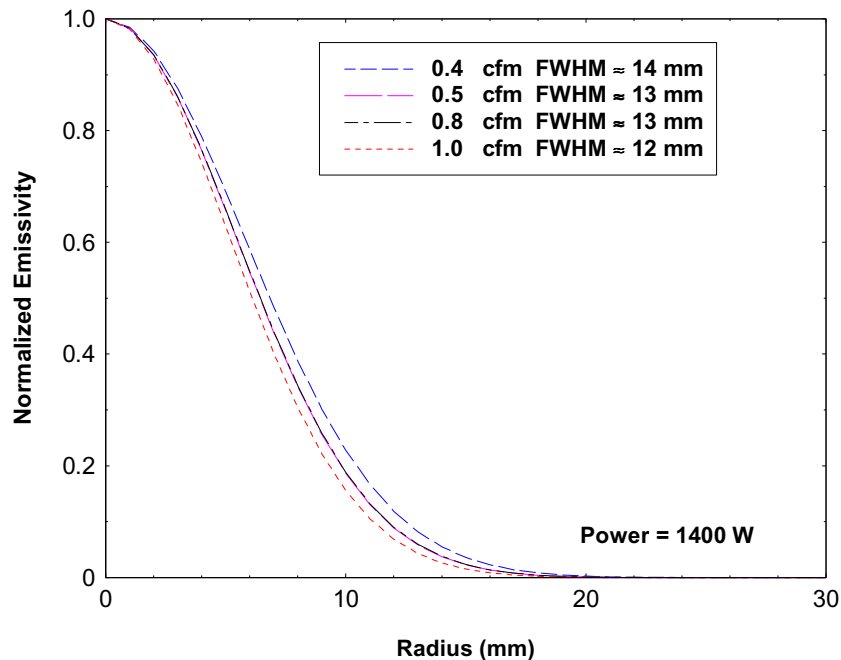


Figure 5.2: Normalized emissivity at constant power with varying flow rate for a representative Fe I transition.

### 5.2.1 Microwave Power Variation

During the microwave power experiments, the total gas flow rate remains constant at 0.5 cfm. As before, the data are collected at three microwave powers, 900 W, 1150 W, and 1400 W, according to the procedures described in Section 4.1. Again the reflected power represents less than 1 % of the forward power.

Using the emissivity profile values determined in Section 5.1.1, the electronic excitation temperature profile is determined for each microwave power level. Figure 5.3 displays these electronic excitation temperature profile results. Increasing the microwave power has no effect, within the error bars of the measurements, on the electronic excitation temperature of the plasma. Similarly, Timofeev has reported that increasing the microwave power by two orders of magnitude produces only a minor effect on the plasma temperature of an atmospheric pressure microwave plasma discharge [33].

In Section 5.1.1, Figure 5.1 shows the plasma diameter growing as the microwave



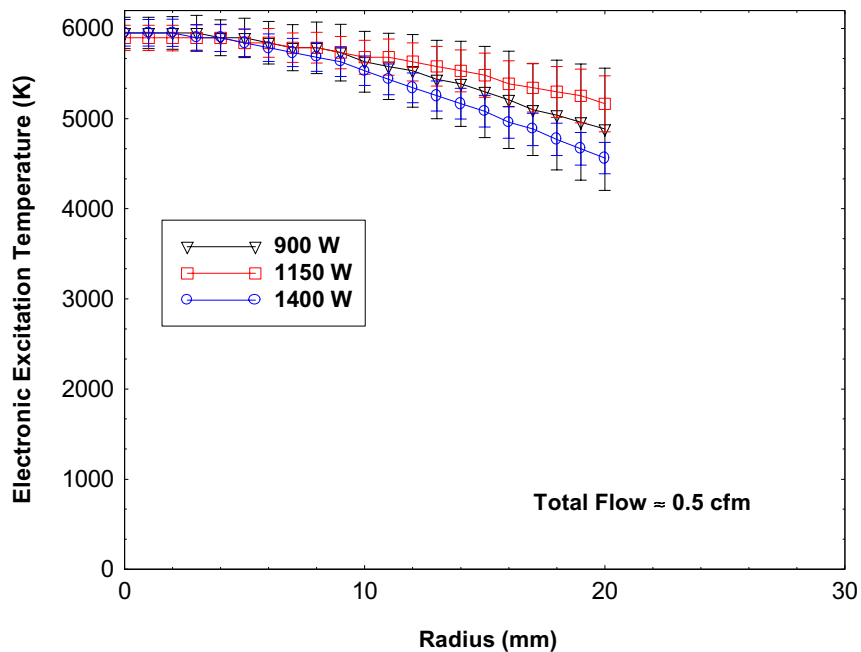


Figure 5.3: Electronic excitation temperature at constant flow with varying microwave power.

power increases. The additional microwave power, therefore, contributes to expanding the plasma volume rather than increasing the plasma’s electronic excitation temperature. The ASTEX power supply capability has limited further investigation of the effect of increasing the microwave power on the expansion of the plasma diameter (see Section 3.1).

## 5.2.2 Gas Flow Rate Variation

The microwave power stays constant at 1400 W with less than 1 % reflected power throughout these total gas flow rate variation experiments. Again the data are collected at four total flow rates, 0.4 cfm, 0.5 cfm, 0.8 cfm, and 1.0 cfm, according to the procedures outlined in Section 4.1. Section 5.1.2 gives the axial and swirl gas flow rates.

Lowering the gas flow rate increases the residence time of sample particles in the plasma. The residence time is defined as the time a particle spends in the plasma dur-

ing which it may become excited (see Section 2.4). Under the assumption of laminar flow, using Equation 2.12 gives the residence time of a particle in a gas flow stream of 0.4 cfm as 6 ms. In a gas flow stream of 1.0 cfm, the residence time is 2 ms. An increased time in the plasma is assumed to increase the probability of exciting the particle for monitoring purposes. Ogura et al. report the lowest electronic excitation values with the highest carrier gas flow rate, since high gas flow rates significantly reduce the residence time [26]. Therefore, examining the electronic excitation temperature profiles in the MP-CEM is expected to confirm that increasing the total gas flow rate cools the plasma.

Utilizing the emissivity values shown in Figure 5.2 allows for the determination of the electronic excitation temperature profiles. Figure 5.4 shows the results of varying the total gas flow rates on the electronic excitation temperature profiles. Instead of confirming the expected result that an increased flow rate cools the plasma electronic excitation temperature, Figure 5.4 shows the reverse.  $T_{exc}$ , in fact, rises with increased total flow rate. The results displayed in Figure 5.4 have proved counterintuitive. Therefore, an effect beyond particle residence time is sought.

The sample particles once volatilized into atomic and molecular species do not travel directly through the plasma. These neutral particles experience numerous collisions with electrons as they traverse the plasma. Equation 2.13 yields the mean free path of electrons,  $\lambda_{MFP}$ , in the plasma. Using the atmospheric pressure neutral gas density for air at 5900 K,  $n_g = 10^{18} \text{ cm}^{-3}$ , and from Timofeev the cross-section for electron scattering by neutral atomic and molecular particles,  $\sigma = 10^{-15} \text{ cm}^2$ , gives a  $\lambda_{MFP}$  of 1 mm [33]. This mean free path is smaller than the 2 cm diameter plasma.

For the following calculations the electronic excitation temperature is assumed to mirror the electron temperature. The collision time of the electrons, given by Equation 2.15, yields a value of 2 ps for electrons with a velocity derived from using an electron temperature of 5900 K (see Section 2.4). Using Equation 2.16 to determine the collision frequency shows that an electron experiences 400 million collisions per second. For a gas flow rate of 0.4 cfm and a residence time of 6 ms in the plasma, an electron experiences 2.5 million collisions while in the driven region of the plasma.

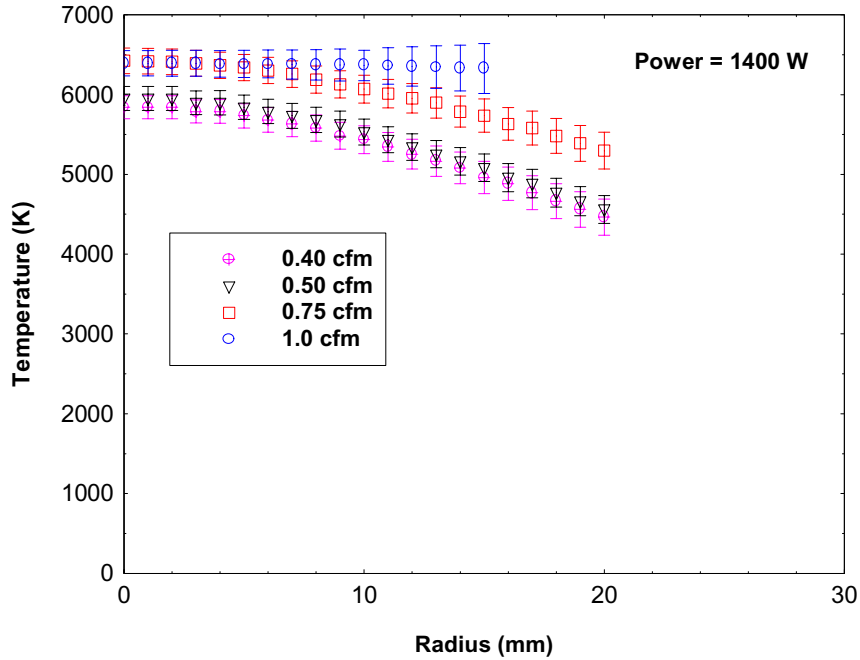


Figure 5.4: Electronic excitation temperature at constant microwave power with varying total gas flow rate.

Likewise, with a gas flow rate of 1.0 cfm, an electron temperature of 6400 K, and a residence time of 2 ms, an electron experiences 800 thousand collisions. Thus collisions of neutral particles with electrons control the dynamics of the atmospheric pressure microwave air plasma. Because of the high collision frequency, the electrons do not have sufficient time between collisions to be accelerated by the microwave field. Thus, the temperature remains nearly constant with a change in the microwave power as seen in Figure 5.3.

These calculations assume an infinite plasma while, in fact, the plasma has a finite size. Figure 5.2 shows that the plasma diameter decreases as the gas flow rate increases. As stated in Section 5.1.2, the plasma volume decreases by  $\sim 25\%$  as the gas flow rate increases from 0.4 cfm to 1.0 cfm. This volume restriction shows a better confined plasma at a high flow rate than at a low flow rate. This improved confinement may, in part, be attributed to a high swirl flow rate in the 1.0 cfm total gas flow rate regime. In the plasma at 1.0 cfm, the improved confinement reduces

thermal losses from the plasma core. Therefore, the electronic excitation temperature increases by  $\sim 10\%$  as the gas flow rate increases from 0.4 cfm to 1.0 cfm as shown in Figure 5.4.

### 5.3 LTE Verification

The electronic excitation temperature calculations require LTE in the plasma (see Section 2.3). Therefore the assumption of LTE is checked.

Under assumptions of LTE,

$$T_e = T_i = T_{exc} \quad (5.1)$$

where all temperatures in the plasma are equal except the blackbody radiation temperature (see Section 2.2) [6].

In Section 5.2,  $T_{exc}$ , on-axis, is reported as  $5800 \text{ K} \pm 200 \text{ K}$  at 0.4 cfm and 1400 W. Borrás has performed preliminary measurements of the rotational temperature in nitrogen in the same MPT system [4]. The rotational temperature approximately equals the gas kinetic temperature or ion temperature. In a similar gas flow rate and power regime, Borrás' results reveal a flat ion temperature profile of  $5400 \text{ K} \pm 400 \text{ K}$  [4]. Matousek et. al. report

$$T_i < T_{exc} \ll T_e \quad (5.2)$$

in the case of no LTE [22]. Unfortunately,  $T_i$  results only exist in this one regime. However, the limited ion temperatures obtained by Borrás agree well with the electronic excitation temperatures measured in Section 5.2. The fact that  $T_i$  equals  $T_{exc}$  implies that the plasma is in LTE. Timofeev also reports an atmospheric pressure microwave plasma nearly in thermodynamic equilibrium [33]. So, an electron temperature of 5800 K is used for the following calculations.

With this  $T_e$ , Equation 2.6 yields an electron density,  $n_e = 1.7 \times 10^{14} \text{ cm}^{-3}$ . As discussed in Section 2.2, the Griem criterion, given by Equation 2.5, allows for the determination of LTE in a plasma. Using  $T_e = 5800 \text{ K}$ , the electron density

must exceed  $1.0 \times 10^{11} \text{ cm}^{-3}$  for the assumption of LTE to remain valid. Since the approximated electron density does exceed this value, this plasma meets the Griem criterion for LTE.

## 5.4 Skin Depth and Conductivity Calculations

As discussed in Section 2.4, the skin depth equation, Equation 2.19, remains valid only if  $\omega_{pe}, \nu_m \gg \omega$  [21]. Using the energy collision frequency determined in Section 5.2.2, Equation 2.17 yields a momentum collision frequency of  $1.1 \times 10^{13} \text{ Hz}$  which greatly exceeds the microwave frequency,  $\omega = 2.45 \times 10^9 \text{ Hz}$ . Relying on the electron density calculated in Section 5.3, Equation 2.18 gives an electron plasma frequency,  $\omega_{pe} = 1.17 \times 10^{11} \text{ Hz}$  which also surpasses  $\omega$ . Therefore, Equation 2.19 is valid in this case for the determination of the skin depth of the microwave frequency,  $\omega = 2.45 \text{ GHz}$ , in the MPT.

In Section 5.1, Figures 5.1 and 5.2 demonstrate that the skin depth for this microwave wavelength in a plasma with an electron density of  $1.7 \times 10^{14} \text{ cm}^{-3}$  must exceed the plasma diameter. Otherwise, the emissivity profiles in these figures would display a hollowing near the center of the plasma. The skin depth for the microwave plasma must exceed 0.7 cm.

Using Equation 2.19, the skin depth of the 2.45 GHz microwave frequency, at the density calculated in Section 5.3, is 24 cm. The uncertainty in the electron-neutral cross-section prevents a more accurate skin depth calculation. However, this value provides an upper limit for the skin depth. Since the reflected microwave power is typically less than 1 % of the forward power, the plasma must absorb most of the microwave energy. Otherwise, the reflected power would be much larger than 1 %. Therefore, the skin depth must be on the order of four plasma radii to allow for even microwave heating of the plasma as seen in Figures 5.3 and 5.4.

From Equation 2.23, the wavelength of the microwaves propagating in the waveguide is 24 cm. This skin depth implies that at this electron density, the plasma size, currently  $\sim 0.7 \text{ cm}$  in diameter, may be increased without adversely affecting

the microwave heating. The microwave wavelength will penetrate a larger plasma and deposit its energy. However, the optical thickness of the plasma must also be considered when rescaling the plasma.

Since the skin depth for the microwave plasma ranges between 0.7 cm and 24 cm, the limits on the plasma conductivity may also be determined. Equation 2.20 gives a plasma conductivity with a range of

$$1.13 \times 10^{-2}(\Omega m)^{-1} < \sigma_{dc} < 13(\Omega m)^{-1}. \quad (5.3)$$

In Section 5.1, Figures 5.1 and 5.2 demonstrate that the plasma is optically thin. Otherwise, the emissivity profiles in these figures would display a hollowing near the center of the plasma. Therefore, the optical wavelengths can penetrate at least 0.7 cm in a microwave plasma with an electron density,  $n_e = 1.7 \times 10^{14} \text{ cm}^{-3}$ . The determination of the size at which the plasma becomes optically thick must be determined experimentally as discussed in Chapter 6.

# Chapter 6

## Future Work

The research presented in this text has begun the characterization of the MPT at MIT. However, a complete understanding of the plasma has not been obtained. Therefore, the following discussion suggests possibilities for further investigation.

### Detection Limit Survey

Section 5.2.2 describes the surprising result that increasing the total gas flow rate causes a rise in the electronic excitation temperature,  $T_{exc}$ . Table 1.1 shows the current detection limits acquired at the gas flow rate of 0.5 cfm. The increase in  $T_{exc}$  should lead to an improvement in the MP-CEM's sensitivity to the trace hazardous metals. Therefore, the detection limits should be redetermined at 1.0 cfm.

### Rotational Temperature Determination

As stated in Section 5.3, Borrás has performed preliminary measurements of the rotational temperature,  $T_{rot}$ , in the MPT. The rotational temperature mirrors the ion gas kinetic temperature [22]. Borrás examines the nitrogen bandlines in the plasma to determine the ion temperature [4]. Distinguishing the nitrogen bandlines from the air plasma background presents many difficulties. Therefore, the working gas in the  $T_{rot}$  measurements made by Borrás is nitrogen instead of air.

Even though nitrogen constitutes 78 % of air, an air plasma differs from a nitro-

gen plasma because of its other constituents [23]. Therefore, rotational temperature measurements in an air plasma would be ideal. Due to the interference of the other species, the nitrogen bandlines cannot be used to calculate  $T_{rot}$  in an air plasma.

Matousek et al. report the use of the rotational lines of the OH band at 306.4 nm for the determination of  $T_{rot}$  [22]. Dieke and Crosswhite have determined the transition probabilities,  $A$ , of the main branches [7]. Using the (0-0) band, the  $Q_1$  branch of OH looks the most promising for ion temperature determination. Wavelengths,  $\lambda$ , in the  $Q_1$  branch fall in the region of 307 nm to 314 nm. The Princeton Instruments detector array is sensitive in this region.

The calculation of  $T_{rot}$  entails plotting  $\log(I\lambda/A)$  versus the line energy where  $I$  is the intensity of the OH line. The slope of a straight line fit through these points relates to the rotational temperature by

$$m = -\frac{0.625}{T_{rot}} \quad (6.1)$$

where  $m$  is the slope of the line [6]. Boumans gives a concise list of the wavelengths, energies, and transition probabilities for the  $Q_1$  branch. In addition to using OH bands for rotational temperature determination, Boumans reports the use of CN, BO, and  $C_2$  bands for this purpose [6].

For comparison, the  $T_{rot}$  profile must be determined in the same microwave power and gas flow rate regimes as the  $T_{exc}$  described in Section 5.2. The outcome of this investigation will verify the existence of LTE throughout the plasma.

## Gas Flow Rate Study

The excitation temperature measurements in Section 5.2.2 focus on the effects of varying the total gas flow rate. However, the individual effects of swirl and axial gas flow rates are neglected. A systematic study in which the axial gas flow rate remains constant and the swirl gas flow rate varies will separate the effects of the two gas flow rates on  $T_{exc}$  and  $T_{rot}$ . Of course, the study should include varying the axial flow rate and maintaining the swirl flow rate.



Additionally, flow rates beyond 1.0 cfm deserve examination as well. To achieve these flow rates requires a high-pressure air source and wide range rotameters. Determining the flow rate at which  $T_{exc}$  reaches its maximum is essential to improving the sensitivity of the MP-CEM to trace hazardous metals.

### **Plasma Scaling**

Section 5.4 discusses the optical thickness of the microwave plasma. At its current size and density, the microwave plasma is optically thin. Therefore, the plasma volume may be increased without impeding the use of spectroscopic diagnostics.

The extent of the possible plasma scaling is uncertain. The skin depth of the microwave frequency in the plasma ranges between 0.7 cm and 24 cm (see Section 5.4). Therefore, a systematic study should be undertaken to find the skin depth of the plasma. This investigation requires increasing the microwave power into the plasma beyond the 1.5 kW capability of the current ASTEX power supply. Figure 5.1 shows that the plasma diameter increases with increased microwave power. Therefore, the cavity which contains the plasma must also be enlarged.

A large plasma volume should allow for the excitation of more of the trace hazardous metals. Therefore, scaling up the size of the plasma may lead to lower detection limits for the metals.

The possibilities for the MPT abound. The studies suggested here barely scratch the surface of the interesting physics questions supplied by the MPT. As a continuous emissions monitor or in its next reincarnation, the MPT will provide an interesting subject for future research.

# Appendix A

## Electric Field Concentration

Section 3.1 mentions that inserting a tungsten, W, wire into the waveguide ignites the microwave plasma. The W wire serves two vital purposes for starting the plasma. First, the W provides a source of electrons needed for ionizing the air. The E-field accelerates the electrons which then collide with the air molecules leading to ionization. Secondly, the W wire concentrates the E-field. Applying Gauss's Theorem to Coulomb's Law yields

$$\begin{aligned}\int_A \underline{E} \cdot d\underline{A} &= \int_V (\nabla \cdot \underline{E}) dV \\ 4\pi r^2 E &= \int_V \frac{\rho}{\epsilon_o} dV \\ 4\pi r^2 E &= \frac{Q}{\epsilon_o} \\ E &= \frac{Q}{4\pi\epsilon_o r^2}\end{aligned}\tag{A.1}$$

where E is the electric field, Q is the charge,  $\epsilon_o$  is the vacuum permittivity constant, and  $r$  is the radius of the W wire. Equation A.1 shows that the electric field is inversely proportional to the radius of the W wire. Therefore, a small diameter wire causes a large E-field to concentrate. To ignite the MPT, a 0.25 mm diameter W wire is used. This wire effectively concentrates the E-field above the  $\sim 15,000$  V/cm needed to breakdown the air.

# Appendix B

## Procedure for Starting the MPT

1. Turn on the cooling water.
2. Open the compressed air valve.
3. Using the needle valve, set the axial gas flow rate to  $\sim 0.5$  cfm.

**NOTE** Equation 3.1 gives the conversion of the Omega flowmeter reading to standard units.

4. Using the needle valve, close the swirl gas flow.
5. Turn on the ASTEX power supply.
6. Set the forward microwave power for 900 W to 1500 W.
7. Send the microwaves down the waveguide by pushing the green button on the power supply.
8. Insert a two pronged W wire into the waveguide cavity until the plasma forms.

**NOTE** Place the W wire in a long ceramic rod with an elbow bend. Upon ignition the plasma will extend quite far. No part of your body should ever be directly over the microwave cavity.

**NOTE** A small diameter W wire works best (see Appendix A).

9. Quickly remove the W wire as soon as the plasma forms.
10. Using the needle valve, adjust the swirl flow rate until the plasma stabilizes.

**NOTE** The plasma should never remain in contact with the quartz cylinder.

11. Adjust the tuning stubs to minimize the reflected power.

**NOTE** The reflected power should never exceed 5 % of the forward power.

Typically, the reflected power is < 1 % of the forward power.

12. Wait 30 minutes while the temperatures of the waveguide and the bronze can equilibrate.
13. Open the nebulizer gas flow at 40 psi.
14. Using the needle valves, set the axial and swirl flow rates for the experiment.

**NOTE** The plasma is not stable for all axial and swirl flow rates. Monitor the reflected power and visually monitor the plasma to ensure stability. Do not allow the reflected power to exceed 5 % of the forward power or the plasma to attach to the quartz cylinder.

15. Wait 15 minutes.
16. Check that the axial and swirl gas flow rates have remained constant. Adjust as needed.
17. Repeat the previous two steps until the flow rates remain constant to within 0.03 cfm.

# Appendix C

## Spyglass Macro

This Spyglass Macro, loop, calls the macros iron09bs and iron10bs. The iron09bs and iron10bs codes average each pixel in the spectrum for the twenty-five raw spectrum files.

### Spyglass Macro - loop

```
call loop(1, 9, 1, "iron09bs")
call loop(10, 158, 1, "iron10bs")
```

### Spyglass Macro - iron09bs

```
user_interactive = false
import_3d = false
import_3daxis = 1
import_coldelim = false
import_byteswap = false
import_delimiter = 3
import_dimcolumns = 513
import_dimrows = 25
import_dimlayers = 1
import_filetype = 8
```

```

import_numtype = 5
import_record = 0
import_skip = 4100
import_transpose = false

call setdirectory("c:\Data\Temperature\Electron\Iron\121599\rawdata")
call setsavedirectory("C:\Data\Temperature\Electron\Iron\121599
\reduced")

*
q = loop_index
*
f = "12fe0"//q//".spe"
*
call open(f)
*
average = colavg(var("_12fe0"//q//"_spe"))
fe = transpose(average)
call setnames("fe","fe"//q,"","")
select = setselection("fe"//q,0,0,0,511)
call extractselection("fe"//q)
call saveas("fe"//q//"_x","fe"//q,3)
*
call closeall

```

### **Spyglass Macro - iron10bs**

```

user_interactive = false
import_3d = false
import_3daxis = 1
import_coldelim = false
import_byteswap = false

```

```

import_delimiter = 3
import_dimcolumns = 513
import_dimrows = 25
import_dimlayers = 1
import_filetype = 8
import_numtype = 5
import_record = 0
import_skip = 4100
import_transpose = false

call setdirectory("c:\Data\Temperature\Electron\Iron\121599\rawdata")
call setsavedirectory("C:\Data\Temperature\Electron\Iron\121599
\reduced")

*
q = loop_index
*
f = "12fe"//q//".spe"
*
call open(f)
*
average = colavg(var("_12fe"//q//"_spe"))
fe = transpose(average)
call setnames("fe","fe"//q,"","")
select = setselection("fe"//q,0,0,0,511)
call extractselection("fe"//q)
call saveas("fe"//q//"_x","fe"//q,3)
*
call closeall

```

# Appendix D

## Excel Macro - Water Subtraction

```
Sub Macro1()  
  
Dim a  
Dim day  
  
day = 121599  
  
For a = 1 To 158 Step 2  
  
    Workbooks.Add  
  
    ChDir "C:\Data\Temperature\Electron\Iron\" & day & "\waterout"  
  
    ActiveWorkbook.SaveAs FileName:= _  
        "C:\Data\Temperature\Electron\Iron\" & day & "\waterout  
        \preabel" & a & ".xls", FileFormat _ :=xlNormal,  
        Password:="", WriteResPassword:="", ReadOnlyRecommended  
        := _ False, CreateBackup:=False  
  
    ChDir "C:\Data\Temperature\Electron\Iron\" & day & "\reduced"
```



```
Workbooks.OpenText FileName:= _  
    "C:\Data\Temperature\Electron\Iron\" & day & "\reduced\fe"  
& a, Origin:=xlWindows, _ StartRow:=1, DataType:=xlDelimited,  
TextQualifier:=xlDoubleQuote, _ ConsecutiveDelimiter:=False,  
Tab:=True, Semicolon:=False, Comma:=False _, Space:=False,  
Other:=False, FieldInfo:=Array(Array(1, 1), Array(2, 1), _  
    Array(3, 1))
```

```
Windows("fe" & a).Activate  
Range("B2:B513").Select  
Selection.Copy
```

```
Windows("calculator.xls").Activate  
Range("A1:A512").Select  
ActiveSheet.Paste
```

```
Windows("fe" & a).Activate  
ActiveWorkbook.Close (False)
```

```
Workbooks.OpenText FileName:= _  
    "C:\Data\Temperature\Electron\Iron\" & day & "\reduced\fe"  
& a + 1, Origin:=xlWindows, _ StartRow:=1, DataType:=  
xlDelimited, TextQualifier:=xlDoubleQuote, _  
ConsecutiveDelimiter:=False, Tab:=True, Semicolon:=False,  
Comma:=False _, Space:=False, Other:=False, FieldInfo:=  
Array(Array(1, 1), Array(2, 1), _ Array(3, 1))
```

```
Windows("fe" & a + 1).Activate
```

```
Range("B2:B513").Select
```

```
Selection.Copy
```

```
Windows("calculator.xls").Activate
```

```
Range("C1:C512").Select
```

```
ActiveSheet.Paste
```

```
Windows("fe" & a + 1).Activate
```

```
ActiveWorkbook.Close (False)
```

```
Windows("calculator.xls").Activate
```

```
Range("D1").Select
```

```
ActiveCell.FormulaR1C1 = "=RC[-3]-RC[-1]"
```

```
Range("D1:D512").Select
```

```
Selection.FillDown
```

```
Range("D1:D512").Select
```

```
Selection.Copy
```

```
Windows("preabel" & a & ".xls").Activate
```

```
Range("A1:A512").Select
```

```
Selection.PasteSpecial Paste:=xlValues, Operation:=xlNone,
```

```
SkipBlanks:= _ False, Transpose:=False
```

```
ChDir "C:\Data\Temperature\Electron\Iron\" & day & "\waterout"
```

```
ActiveWorkbook.Save
```

```
ActiveWorkbook.Close (False)
```

```
Workbooks.Add
```

```
ActiveWorkbook.Close (False)
```

```
Next a
```

```
End Sub
```

# Appendix E

## Excel Macro - Pixel Determination

```
Sub Macro1()  
,  
' Macro1 Macro  
' Macro recorded 1/30/99 by Karyn M. Green  
,  
  
Dim b  
Dim c  
Dim d  
Dim numfile  
Dim day  
Dim line682  
Dim line684  
Dim line701  
Dim line704  
Dim line719  
Dim line724  
Dim line727  
Dim line732  
Dim line734  
Dim line737
```

Dim line738

Dim line748

Dim line749

Dim line758

Dim line760

Dim line763

Dim line765

Dim line767

' day is the date directory in which the data files are located

day = 121599

' numfile is the number of preabel files

numfile = 79

' example of variable line724 stands for line 372.4 nm

' for each variable line000 put in the center pixel of that peak

' if there is no pixel set that variable to 0

line682 = 0

line684 = 0

line701 = 0

line704 = 0

line719 = 420

line724 = 386

line727 = 362

line732 = 326

line734 = 307

line737 = 290

line738 = 0

```
line748 = 205
line749 = 196
line758 = 130
line760 = 116
line763 = 87
line765 = 74
line767 = 61
```

```
ChDir "C:\Data\Temperature\Electron\Iron\" & day & "\waterout"
```

```
Workbooks.Open FileName:= _
    "C:\Data\Temperature\Electron\Iron\" & day & "\ezplots
    \ezdata.xls"
```

```
Windows("abeldata.xls").Activate
```

```
Range("A1").Select
ActiveCell.FormulaR1C1 = "=0"
```

```
Range("A2").Select
ActiveCell.FormulaR1C1 = "=1+R[-1]C"
```

```
Range("A2").Select
Selection.Copy
```

```
Range("A2:A" & numfile + 1).Select
ActiveSheet.Paste
```

```
For c = 1 To numfile Step 1
```

```

Windows("abedata.xls").Activate
b = c + Range("A" & c).Value

Workbooks.Open FileName:= _
    "preabel" & b & ".xls"

Windows("preabel" & b & ".xls").Activate

If line682 > 0 Then
    If Range("A" & line682 - 1).Value > Range("A" & line682).
        Value Then
            If Range("A" & line682 - 1).Value > Range
                ("A" & line682 + 1).Value Then
                    Range("A" & line682 - 1).Select
                    Selection.Copy
                    Windows("ezdata.xls").Activate
                    Range("C" & c + 1).Select
                    ActiveSheet.Paste
                    GoTo 100
            End If
        End If
    End If

Windows("preabel" & b & ".xls").Activate
If Range("A" & line682) > Range("A" & line682 + 1) Then
    Range("A" & line682).Select
    Selection.Copy
    Windows("ezdata.xls").Activate
    Range("C" & c + 1).Select
    ActiveSheet.Paste

```

GoTo 100

End If

Windows("preabel" & b & ".xls").Activate

If Range("A" & line682) < Range("A" & line682 + 1) Then

    Range("A" & line682 + 1).Select

    Selection.Copy

    Windows("ezdata.xls").Activate

    Range("C" & c + 1).Select

    ActiveSheet.Paste

    GoTo 100

End If

100 End If

Windows("preabel" & b & ".xls").Activate

If line684 > 0 Then

    If Range("A" & line684 - 1).Value > Range("A" & line684) Then

        If Range("A" & line684 - 1).Value > Range

            ("A" & line684 + 1) Then

            Range("A" & line684 - 1).Select

            Selection.Copy

            Windows("ezdata.xls").Activate

            Range("D" & c + 1).Select

            ActiveSheet.Paste

            GoTo 200

        End If

    End If

Windows("preabel" & b & ".xls").Activate



```
If Range("A" & line684) > Range("A" & line684 + 1) Then
    Range("A" & line684).Select
    Selection.Copy
    Windows("ezdata.xls").Activate
    Range("D" & c + 1).Select
    ActiveSheet.Paste
    GoTo 200
End If
```

```
Windows("preabel" & b & ".xls").Activate
    Range("A" & line684 + 1).Select
    Selection.Copy
    Windows("ezdata.xls").Activate
    Range("D" & c + 1).Select
    ActiveSheet.Paste
```

```
200 End If
```

```
Windows("preabel" & b & ".xls").Activate
```

```
If line701 > 0 Then
```

```
    If Range("A" & line701 - 1).Value > Range("A" & line701)
```

```
        Then
```

```
            If Range("A" & line701 - 1).Value > Range
```

```
                ("A" & line701 + 1) Then
```

```
                    Range("A" & line701 - 1).Select
```

```
                    Selection.Copy
```

```
                    Windows("ezdata.xls").Activate
```

```
                    Range("E" & c + 1).Select
```

```
                    ActiveSheet.Paste
```

```

        GoTo 300
    End If
End If

Windows("preabel" & b & ".xls").Activate
If Range("A" & line701) > Range("A" & line701 + 1) Then
    Range("A" & line701).Select
    Selection.Copy
    Windows("ezdata.xls").Activate
    Range("E" & c + 1).Select
    ActiveSheet.Paste
    GoTo 300
End If

Windows("preabel" & b & ".xls").Activate
    Range("A" & line701 + 1).Select
    Selection.Copy
    Windows("ezdata.xls").Activate
    Range("E" & c + 1).Select
    ActiveSheet.Paste
300 End If

Windows("preabel" & b & ".xls").Activate

If line704 > 0 Then
    If Range("A" & line704 - 1).Value > Range("A" & line704) Then
        If Range("A" & line704 - 1).Value > Range
            ("A" & line704 + 1) Then
                Range("A" & line704 - 1).Select

```

```

        Selection.Copy
        Windows("ezdata.xls").Activate
        Range("F" & c + 1).Select
        ActiveSheet.Paste
        GoTo 400
    End If
End If

    If Range("A" & line704) > Range("A" & line704 + 1)
    Then
        Range("A" & line704).Select
        Selection.Copy
        Windows("ezdata.xls").Activate
        Range("F" & c + 1).Select
        ActiveSheet.Paste
        GoTo 400
    End If

        Range("A" & line704 + 1).Select
        Selection.Copy
        Windows("ezdata.xls").Activate
        Range("F" & c + 1).Select
        ActiveSheet.Paste
400 End If

Windows("preabel" & b & ".xls").Activate

```

```

If line719 > 0 Then
    If Range("A" & line719 - 1).Value > Range("A" & line719) Then
        If Range("A" & line719 - 1).Value > Range
            ("A" & line719 + 1) Then
                Range("A" & line719 - 1).Select
                Selection.Copy
                Windows("ezdata.xls").Activate
                Range("G" & c + 1).Select
                ActiveSheet.Paste
                GoTo 500
            End If
        End If
    End If

    If Range("A" & line719) > Range("A" & line719 + 1)
        Then
            Range("A" & line719).Select
            Selection.Copy
            Windows("ezdata.xls").Activate
            Range("G" & c + 1).Select
            ActiveSheet.Paste
            GoTo 500
        End If

        Range("A" & line719 + 1).Select
        Selection.Copy
        Windows("ezdata.xls").Activate
        Range("G" & c + 1).Select
        ActiveSheet.Paste
    End If

500 End If

```

```
Windows("preabel" & b & ".xls").Activate
```

```
If line724 > 0 Then
```

```
    If Range("A" & line724 - 1).Value > Range("A" & line724) Then
```

```
        If Range("A" & line724 - 1).Value > Range
```

```
            ("A" & line724 + 1) Then
```

```
                Range("A" & line724 - 1).Select
```

```
                Selection.Copy
```

```
                Windows("ezdata.xls").Activate
```

```
                Range("H" & c + 1).Select
```

```
                ActiveSheet.Paste
```

```
                GoTo 600
```

```
            End If
```

```
        End If
```

```
    If Range("A" & line724) > Range("A" & line724 + 1)
```

```
    Then
```

```
        Range("A" & line724).Select
```

```
        Selection.Copy
```

```
        Windows("ezdata.xls").Activate
```

```
        Range("H" & c + 1).Select
```

```
        ActiveSheet.Paste
```

```
        GoTo 600
```

```
    End If
```

```
        Range("A" & line724 + 1).Select
```

```
        Selection.Copy
```

```
        Windows("ezdata.xls").Activate
```

```
        Range("H" & c + 1).Select
```

ActiveSheet.Paste

600 End If

Windows("preabel" & b & ".xls").Activate

If line727 > 0 Then

If Range("A" & line727 - 1).Value > Range("A" & line727) Then

If Range("A" & line727 - 1).Value > Range

("A" & line727 + 1) Then

Range("A" & line727 - 1).Select

Selection.Copy

Windows("ezdata.xls").Activate

Range("I" & c + 1).Select

ActiveSheet.Paste

GoTo 700

End If

End If

If Range("A" & line727) > Range("A" & line727 + 1)

Then

Range("A" & line727).Select

Selection.Copy

Windows("ezdata.xls").Activate

Range("I" & c + 1).Select

ActiveSheet.Paste

GoTo 700

End If

Range("A" & line727 + 1).Select

```

        Selection.Copy
        Windows("ezdata.xls").Activate
        Range("I" & c + 1).Select
        ActiveSheet.Paste
700 End If

Windows("preabel" & b & ".xls").Activate

If line732 > 0 Then
    If Range("A" & line732 - 1).Value > Range("A" & line732) Then
        If Range("A" & line732 - 1).Value > Range
            ("A" & line732 + 1) Then
                Range("A" & line732 - 1).Select
                Selection.Copy
                Windows("ezdata.xls").Activate
                Range("J" & c + 1).Select
                ActiveSheet.Paste
                GoTo 800
            End If
        End If
    End If

    If Range("A" & line732) > Range("A" & line732 + 1)
    Then
        Range("A" & line732).Select
        Selection.Copy
        Windows("ezdata.xls").Activate
        Range("J" & c + 1).Select
        ActiveSheet.Paste
        GoTo 800
    End If

```

End If

```
Range("A" & line732 + 1).Select
Selection.Copy
Windows("ezdata.xls").Activate
Range("J" & c + 1).Select
ActiveSheet.Paste
```

800 End If

```
Windows("preabel" & b & ".xls").Activate
```

```
If line734 > 0 Then
```

```
  If Range("A" & line734 - 1).Value > Range("A" & line734) Then
```

```
    If Range("A" & line734 - 1).Value > Range
```

```
      ("A" & line734 + 1) Then
```

```
        Range("A" & line734 - 1).Select
```

```
        Selection.Copy
```

```
        Windows("ezdata.xls").Activate
```

```
        Range("K" & c + 1).Select
```

```
        ActiveSheet.Paste
```

```
        GoTo 900
```

```
      End If
```

```
    End If
```

```
  If Range("A" & line734) > Range("A" & line734 + 1)
```

```
  Then
```

```
    Range("A" & line734).Select
```

```
    Selection.Copy
```

```
    Windows("ezdata.xls").Activate
```



```

        Range("K" & c + 1).Select
        ActiveSheet.Paste
        GoTo 900
    End If

        Range("A" & line734 + 1).Select
        Selection.Copy
        Windows("ezdata.xls").Activate
        Range("K" & c + 1).Select
        ActiveSheet.Paste
900 End If

Windows("preabel" & b & ".xls").Activate

If line737 > 0 Then
    If Range("A" & line737 - 1).Value > Range("A" & line737) Then
        If Range("A" & line737 - 1).Value > Range
            ("A" & line737 + 1) Then
                Range("A" & line737 - 1).Select
                Selection.Copy
                Windows("ezdata.xls").Activate
                Range("L" & c + 1).Select
                ActiveSheet.Paste
                GoTo 1000
            End If
        End If
    End If

    If Range("A" & line737) > Range("A" & line737 + 1)
    Then

```

```

        Range("A" & line737).Select
        Selection.Copy
        Windows("ezdata.xls").Activate
        Range("L" & c + 1).Select
        ActiveSheet.Paste
        GoTo 1000
    End If

        Range("A" & line737 + 1).Select
        Selection.Copy
        Windows("ezdata.xls").Activate
        Range("L" & c + 1).Select
        ActiveSheet.Paste
1000 End If

Windows("preabel" & b & ".xls").Activate

If line738 > 0 Then
    If Range("A" & line738 - 1).Value > Range("A" & line738)
    Then
        If Range("A" & line738 - 1).Value > Range
            ("A" & line738 + 1) Then
                Range("A" & line738 - 1).Select
                Selection.Copy
                Windows("ezdata.xls").Activate
                Range("M" & c + 1).Select
                ActiveSheet.Paste
                GoTo 1100
            End If
    End If

```

End If

If Range("A" & line738) > Range("A" & line738 + 1)

Then

Range("A" & line738).Select

Selection.Copy

Windows("ezdata.xls").Activate

Range("M" & c + 1).Select

ActiveSheet.Paste

GoTo 1100

End If

Range("A" & line738 + 1).Select

Selection.Copy

Windows("ezdata.xls").Activate

Range("M" & c + 1).Select

ActiveSheet.Paste

1100 End If

Windows("preabel" & b & ".xls").Activate

If line748 > 0 Then

If Range("A" & line748 - 1).Value > Range("A" & line748).

Value Then

If Range("A" & line748 - 1).Value > Range

("A" & line748 + 1).Value Then

Range("A" & line748 - 1).Select

Selection.Copy

Windows("ezdata.xls").Activate

```

        Range("N" & c + 1).Select
        ActiveSheet.Paste
        GoTo 1200
    End If
End If

If Range("A" & line748).Value > Range("A" & line748 + 1).
    Value Then
    Range("A" & line748).Select
    Selection.Copy
    Windows("ezdata.xls").Activate
    Range("N" & c + 1).Select
    ActiveSheet.Paste
    GoTo 1200
End If

    Range("A" & line748 + 1).Select
    Selection.Copy
    Windows("ezdata.xls").Activate
    Range("N" & c + 1).Select
    ActiveSheet.Paste
1200 End If

Windows("preabel" & b & ".xls").Activate

If line749 > 0 Then
    If Range("A" & line749 - 1).Value > Range("A" & line749) Then
        If Range("A" & line749 - 1).Value > Range
            ("A" & line749 + 1) Then

```

```

        Range("A" & line749 - 1).Select
        Selection.Copy
        Windows("ezdata.xls").Activate
        Range("O" & c + 1).Select
        ActiveSheet.Paste
        GoTo 1300
    End If
End If

Windows("preabel" & b & ".xls").Activate
If Range("A" & line749) > Range("A" & line749 + 1) Then
    Range("A" & line749).Select
    Selection.Copy
    Windows("ezdata.xls").Activate
    Range("O" & c + 1).Select
    ActiveSheet.Paste
    GoTo 1300
End If

Windows("preabel" & b & ".xls").Activate
If Range("A" & line749) < Range("A" & line749 + 1) Then
    Range("A" & line749 + 1).Select
    Selection.Copy
    Windows("ezdata.xls").Activate
    Range("O" & c + 1).Select
    ActiveSheet.Paste
    GoTo 1300
End If
1300 End If

```

```
Windows("preabel" & b & ".xls").Activate
```

```
If line758 > 0 Then
```

```
    If Range("A" & line758 - 1).Value > Range("A" & line758)
```

```
    Then
```

```
        If Range("A" & line758 - 1).Value > Range
```

```
            ("A" & line758 + 1) Then
```

```
                Range("A" & line758 - 1).Select
```

```
                Selection.Copy
```

```
                Windows("ezdata.xls").Activate
```

```
                Range("P" & c + 1).Select
```

```
                ActiveSheet.Paste
```

```
                GoTo 1400
```

```
            End If
```

```
    End If
```

```
    If Range("A" & line758) > Range("A" & line758 + 1)
```

```
    Then
```

```
        Range("A" & line758).Select
```

```
        Selection.Copy
```

```
        Windows("ezdata.xls").Activate
```

```
        Range("P" & c + 1).Select
```

```
        ActiveSheet.Paste
```

```
        GoTo 1400
```

```
    End If
```

```
        Range("A" & line758 + 1).Select
```

```
        Selection.Copy
```

```
        Windows("ezdata.xls").Activate
```

```

Range("P" & c + 1).Select
ActiveSheet.Paste

1400 End If

Windows("preabel" & b & ".xls").Activate

If line760 > 0 Then
  If Range("A" & line760 - 1).Value > Range("A" & line760)
  Then
    If Range("A" & line760 - 1).Value > Range
      ("A" & line760 + 1) Then
        Range("A" & line760 - 1).Select
        Selection.Copy
        Windows("ezdata.xls").Activate
        Range("Q" & c + 1).Select
        ActiveSheet.Paste
        GoTo 1500
      End If
    End If
  End If

  If Range("A" & line760) > Range("A" & line760 + 1)
  Then
    Range("A" & line760).Select
    Selection.Copy
    Windows("ezdata.xls").Activate
    Range("Q" & c + 1).Select
    ActiveSheet.Paste
    GoTo 1500
  End If

```

```

        Range("A" & line760 + 1).Select
        Selection.Copy
        Windows("ezdata.xls").Activate
        Range("Q" & c + 1).Select
        ActiveSheet.Paste
1500 End If

Windows("preabel" & b & ".xls").Activate

If line763 > 0 Then
    If Range("A" & line763 - 1).Value > Range("A" & line763)
    Then
        If Range("A" & line763 - 1).Value > Range
            ("A" & line763 + 1) Then
                Range("A" & line763 - 1).Select
                Selection.Copy
                Windows("ezdata.xls").Activate
                Range("R" & c + 1).Select
                ActiveSheet.Paste
                GoTo 1600
            End If
        End If
    End If

    If Range("A" & line763) > Range("A" & line763 + 1)
    Then
        Range("A" & line763).Select
        Selection.Copy
        Windows("ezdata.xls").Activate
    
```



```

        Range("R" & c + 1).Select
        ActiveSheet.Paste
        GoTo 1600
    End If

        Range("A" & line763 + 1).Select
        Selection.Copy
        Windows("ezdata.xls").Activate
        Range("R" & c + 1).Select
        ActiveSheet.Paste
1600 End If

Windows("preabel" & b & ".xls").Activate

If line765 > 0 Then
    If Range("A" & line765 - 1).Value > Range("A" & line765) Then
        If Range("A" & line765 - 1).Value > Range
            ("A" & line765 + 1) Then
                Range("A" & line765 - 1).Select
                Selection.Copy
                Windows("ezdata.xls").Activate
                Range("S" & c + 1).Select
                ActiveSheet.Paste
                GoTo 1700
            End If
        End If
    End If

    If Range("A" & line765) > Range("A" & line765 + 1)
    Then

```

```
Range("A" & line765).Select
Selection.Copy
Windows("ezdata.xls").Activate
Range("S" & c + 1).Select
ActiveSheet.Paste
GoTo 1700
End If
```

```
Range("A" & line765 + 1).Select
Selection.Copy
Windows("ezdata.xls").Activate
Range("S" & c + 1).Select
ActiveSheet.Paste
```

```
1700 End If
```

```
Windows("preabel" & b & ".xls").Activate
```

```
If line767 > 0 Then
```

```
  If Range("A" & line767 - 1).Value > Range("A" & line767) Then
```

```
    If Range("A" & line767 - 1).Value > Range
```

```
      ("A" & line767 + 1) Then
```

```
        Range("A" & line767 - 1).Select
```

```
        Selection.Copy
```

```
        Windows("ezdata.xls").Activate
```

```
        Range("T" & c + 1).Select
```

```
        ActiveSheet.Paste
```

```
        GoTo 1800
```

```
    End If
```

```
End If
```

```
Windows("preabel" & b & ".xls").Activate
```

```
If Range("A" & line767) > Range("A" & line767 + 1) Then
```

```
    Range("A" & line767).Select
```

```
    Selection.Copy
```

```
    Windows("ezdata.xls").Activate
```

```
    Range("T" & c + 1).Select
```

```
    ActiveSheet.Paste
```

```
    GoTo 1800
```

```
End If
```

```
Windows("preabel" & b & ".xls").Activate
```

```
If Range("A" & line767 + 1) > Range("A" & line767) Then
```

```
    Range("A" & line767 + 1).Select
```

```
    Selection.Copy
```

```
    Windows("ezdata.xls").Activate
```

```
    Range("T" & c + 1).Select
```

```
    ActiveSheet.Paste
```

```
    GoTo 1800
```

```
End If
```

```
1800 End If
```

```
Windows("preabel" & b & ".xls").Activate
```

```
ActiveWindow.Close
```

```
Next c
```

```
Windows("ezdata.xls").Activate
```

```
Cells.Select
```

```
Selection.ColumnWidth = 10.11
```

```
Rows("1:1").Select
```

```
With Selection
```

```
    .HorizontalAlignment = xlCenter
```

```
    .VerticalAlignment = xlBottom
```

```
    .WrapText = False
```

```
    .Orientation = 0
```

```
    .ShrinkToFit = False
```

```
    .MergeCells = False
```

```
End With
```

```
Range("B2").Select
```

```
ActiveCell.FormulaR1C1 = "=0"
```

```
Range("B3").Select
```

```
ActiveCell.FormulaR1C1 = "=1+R[-1]C"
```

```
Range("B3").Select
```

```
Selection.Copy
```

```
Range("B3:B" & numfile + 1).Select
```

```
ActiveSheet.Paste
```

```
For d = 1 To numfile Step 1
```

```
    Range("A" & d + 1).Select
```

```
    ActiveCell.FormulaR1C1 = "preabel" & d + Range("B" & d + 1).Value
```

```
Next d
```

```
    Range("B2").Select
```

```
    ActiveCell.FormulaR1C1 = "=0"
```

```
    Range("B3").Select
```

```
    ActiveCell.FormulaR1C1 = "=1+R[-1]C"
```

```
    Range("B3").Select
```

```
    Selection.Copy
```

```
    Range("B3:B" & numfile + 1).Select
```

```
    ActiveSheet.Paste
```

```
    Range("A1").Select
```

```
    ActiveCell.FormulaR1C1 = "filename"
```

```
    Range("B1").Select
```

```
    ActiveCell.FormulaR1C1 = "chord"
```

```
Range("C1").Select
ActiveCell.FormulaR1C1 = "368.222 nm"

Range("D1").Select
ActiveCell.FormulaR1C1 = "368.411 nm"

Range("E1").Select
ActiveCell.FormulaR1C1 = "370.108 nm"

Range("F1").Select
ActiveCell.FormulaR1C1 = "370.446 nm"

Range("G1").Select
ActiveCell.FormulaR1C1 = "371.993 nm"

Range("H1").Select
ActiveCell.FormulaR1C1 = "372.438 nm"

Range("I1").Select
ActiveCell.FormulaR1C1 = "372.762 nm"

Range("J1").Select
ActiveCell.FormulaR1C1 = "373.239 nm"

Range("K1").Select
ActiveCell.FormulaR1C1 = "373.486 nm"

Range("L1").Select
ActiveCell.FormulaR1C1 = "373.713 nm"
```

```
Range("M1").Select  
ActiveCell.FormulaR1C1 = "373.830 nm"
```

```
Range("N1").Select  
ActiveCell.FormulaR1C1 = "374.826 nm"
```

```
Range("O1").Select  
ActiveCell.FormulaR1C1 = "374.948 nm"
```

```
Range("P1").Select  
ActiveCell.FormulaR1C1 = "375.823 nm"
```

```
Range("Q1").Select  
ActiveCell.FormulaR1C1 = "376.005 nm"
```

```
Range("R1").Select  
ActiveCell.FormulaR1C1 = "376.379 nm"
```

```
Range("S1").Select  
ActiveCell.FormulaR1C1 = "376.554 nm"
```

```
Range("T1").Select  
ActiveCell.FormulaR1C1 = "376.719 nm"
```

```
ActiveWorkbook.Save
```

```
End Sub
```

# Appendix F

## Derivations

### F.1 Radial Emissivity

The radial emissivity,  $\varepsilon(r)$ , relates to the line-integrated intensity,  $I(y)$ , by

$$\varepsilon(r) = -\frac{1}{\pi} \int_r^R \frac{\frac{dI(y)}{dy}}{\sqrt{y^2 - r^2}} dy \quad (\text{F.1})$$

where  $y$  and  $r$  are in Cartesian and radial coordinates respectively. The derivative with respect to  $y$  of Equation 4.3, the Gaussian fit to the intensity data, is given by

$$\frac{dI(y)}{dy} = -2Ab y e^{-by^2} \quad (\text{F.2})$$

where  $A$  and  $b$  are fitting parameters unique to every iron line intensity profile. Plugging Equation F.2 into Equation F.1 yields

$$\varepsilon(r) = \frac{2}{\pi} A b \int_r^R \frac{e^{-by^2}}{\sqrt{y^2 - r^2}} y dy. \quad (\text{F.3})$$

Through the substitution  $u^2 = b(y^2 - r^2)$ , Equation F.3 becomes

$$\varepsilon(r) = \frac{2}{\pi} A b^{\frac{1}{2}} e^{-br^2} \int_0^{\sqrt{b(R^2 - r^2)}} e^{-u^2} du. \quad (\text{F.4})$$



Knowing that the error function,  $\text{erf}(x)$ , has the form

$$\text{erf}(x) = \frac{2}{\sqrt{\pi}} \int_0^x e^{-v^2} dv \quad (\text{F.5})$$

Equation F.4 yields

$$\varepsilon(r) = \frac{1}{\sqrt{\pi}} A b^{\frac{1}{2}} e^{-br^2} \text{erf}([b(R^2 - r^2)]^{\frac{1}{2}}) \quad (\text{F.6})$$

the derived radial emissivity.

## F.2 Reconstructed Intensity

The reconstructed intensity,  $I(y)_{rec}$ , relates to the radial emissivity,  $\varepsilon(r)$ , by

$$I(y)_{rec} = 2 \int_y^R \frac{\varepsilon(r)}{\sqrt{r^2 - y^2}} r dr \quad (\text{F.7})$$

where Equation F.6 gives  $\varepsilon(r)$ . Plugging the derived radial emissivity, Equation F.6, into Equation F.7 gives

$$I(y)_{rec} = \frac{2}{\sqrt{\pi}} A b^{\frac{1}{2}} \int_y^R \frac{\text{erf}([b(R^2 - r^2)]^{\frac{1}{2}})}{\sqrt{r^2 - y^2}} e^{-br^2} r dr. \quad (\text{F.8})$$

Through the substitution,  $x^2 = b(r^2 - y^2)$ , Equation F.8 becomes

$$I_{rec}(y) = \frac{2}{\sqrt{\pi}} A e^{-by^2} \int_0^{\sqrt{b(R^2 - y^2)}} e^{-x^2} \text{erf}([b(R^2 - y^2) - x^2]^{\frac{1}{2}}) dx \quad (\text{F.9})$$

which is not solvable by analytic means. Appendix G shows the code developed to solve Equation F.9 numerically.

# Appendix G

## Excel Macro - Intensity

### Reconstruction

```
Sub erf()  
,  
' erf Macro  
' Macro recorded 6/10/99 by Karyn M. Green  
,
```

Dim A

Dim b

Dim R

Dim y

Dim u

Dim h

Dim Day

Dim umax

Dim c

Dim total

Dim t

Dim s

' Day is the date directory in which erf is located

Day = 40699

' R is the max radius of the plasma

R = 30

' h is the step size between the chords

h = 0.001

A = 4015

b = 0.0346

ChDir "C:\Data\Temperature\Electron\Iron\" & Day & "\ezplots"

Workbooks.Open FileName:= \_

"C:\Data\Temperature\Electron\Iron\" & Day &

"\ezplots\erf.xls"

Workbooks.Open FileName:= \_

"C:\Data\Temperature\Electron\Iron\loop.xls"

Windows("erf.xls").Activate

Columns("A:D").Select

Selection.Copy

Windows("loop.xls").Activate

Columns("A:D").Select

```
ActiveSheet.Paste
```

```
s = 0
```

```
For y = 0 To R Step h
```

```
Windows("loop.xls").Activate
```

```
Columns("E:F").Select
```

```
Selection.ClearContents
```

```
umax = (b * (R ^ 2 - y ^ 2)) ^ 0.5
```

```
t = 0
```

```
For u = 0 To umax Step h
```

```
Windows("loop.xls").Activate
```

```
t = t + 1
```

```
If umax ^ 2 - u ^ 2 < 27 Then
```

```
Range("E" & t).Select
```

```
ActiveCell.FormulaR1C1 = _
```

```
"=exp(-1*" & u & "^2)*erf(sqrt(" & umax & "^2-" & u & "^2))  
*" & h
```

```
GoTo 100
```

```
End If
```

```
Range("E" & t).Select
```

```
ActiveCell.FormulaR1C1 = _
```

```
"=exp(-1*" & u & "^2)*" & h
```

```
100 Next u
```

```
s = s + 1
```

```
Range("F1").Select
```

```
ActiveCell.FormulaR1C1 = _
```

```
"=((2/sqrt(pi()))*" & A & "*exp(-1*" & b & "*" & y & "^2)  
*sum(C[-1]))"
```

```
total = Range("F1").Value
```

```
Windows("erf.xls").Activate
```

```
Range("C" & s).Select
```

```
ActiveCell.FormulaR1C1 = "=" & total
```

```
ActiveWorkbook.Save
```

```
Next y
```

```
ActiveWorkbook.Save
```

```
,
```

```
End Sub
```

# Bibliography

- [1] M. H. Abdallah and J. M. Mermet. The behavior of nitrogen excited in an inductively coupled argon plasma. *J. Quant. Spectrosc. Radiat. Transfer*, 19:83–91, 1978.
- [2] M. H. Abdallah and J. M. Mermet. Comparison of temperature measurements in ICP and MIP with Ar and He as plasma gas. *Spectrochimica Acta B*, 37(5):391–397, 1982.
- [3] J. F. Alder, R. M. Bombelka, and G. F. Kirkbright. Electronic excitation and ionization temperature measurements in a high frequency inductively coupled argon plasma source and the influence of water vapour on plasma parameters. *Spectrochimica Acta. B*, 35:163–175, 1980.
- [4] M. C. Borrás, K. Hadidi, P. Woskov, K. M. Green, G. J. Flores, and P. Thomas. An experiment for radial temperature profile measurements in a microwave induced plasma at atmospheric pressure. IEEE Conference, Raleigh, NC, April 1998.
- [5] M. I. Boulos. The inductively coupled R.F. (radio frequency) plasma. *Pure & Appl. Chem.*, 57(9):1321–1352, 1985.
- [6] P. W. J. M. Boumans, editor. *Chemical Analysis*. 90. John Wiley & Sons, Inc., New York, 1987. Chapters 10-11.
- [7] G. H. Dieke and H. M. Crosswhite. The ultraviolet bands of OH. *Journal of Quantitative Spectroscopy Radiation Transfer*, 2(97):97–199, 1962.

- [8] C. Elachi. *Introduction to the Physics and Techniques of Remote Sensing*. John Wiley & Sons, Inc., New York, 1987.
- [9] U. S. EPA. Determination of metals emissions from stationary sources. Technical report, U.S. Environmental Protection Agency, April 1996. 40 CFR 60 Appendix A.
- [10] U. S. EPA. Specifications and test procedures for multi-metals continuous monitoring systems in stationary sources. Revised standards for hazardous waste combustors, performance specification 10, U.S. Environmental Protection Agency, April 1996. 61 FR 17499 - 17502.
- [11] K. Fallgatter, V. Svoboda, and J. D. Winefordner. Physical and analytical aspects of a microwave excited plasma. *Applied Spectroscopy*, 25(3):347–352, 1971.
- [12] G. J. Flores. Establishing a calibration for a microwave plasma continuous emissions monitor. Master's thesis, Massachusetts Institute of Technology, Nuclear Engineering Department, 1998.
- [13] K. A. Forbes, E. E. Reszke, P. C. Uden, and R. M. Barnes. Comparison of microwave-induced plasma sources. *J. of Analytical Atomic Spectrometry*, 6:57–71, February 1991.
- [14] A. M. Gomes, J. Bacri, J. P. Sarrette, and J. Salon. Measurement of heavy particle temperature in a radiofrequency air discharge at atmospheric pressure from the numerical simulation of the NO  $\gamma$  system. *Journal of Analytical Atomic Spectrometry*, 7:1103–1109, October 1992.
- [15] K. M. Green. Comparison of sample introduction methods in a microwave plasma torch. Bachelor's thesis, Massachusetts Institute of Technology, Nuclear Engineering Department, 1995.
- [16] H. R. Griem. *Plasma Spectroscopy*. McGraw-Hill Book Company, New York, 1964.

- [17] I. H. Hutchinson. *Principles of Plasma Diagnostics*. Cambridge University Press, Cambridge, 1994.
- [18] I. H. Hutchinson. Introduction to plasma physics, September 1997. Class notes for course at the Massachusetts Institute of Technology.
- [19] G. R. Kornblum and L. de Galen. Arrangement for measuring spatial distributions in an argon induction coupled RF plasma. *Spectrochimica Acta B*, 29:249–261, 1974.
- [20] R. L. Liboff. *Introductory Quantum Mechanics*. Addison-Wesley Publishing Company, Reading, Massachusetts, second edition, 1993.
- [21] M. A. Lieberman and A. J. Lichtenberg. *Principles of Plasma Discharges and Materials Processing*. John Wiley & Sons, Inc., New York, 1994.
- [22] J. P. Matousek, B. J. Orr, and M. Selby. Microwave-induced plasmas: Implementation and application. *Prog. analyt. atom. Spectrosc.*, 7:275–314, 1984.
- [23] D. A. McQuarrie and P. A. Rock. *General Chemistry*. W. H. Freeman and Company, New York, third edition, 1991.
- [24] K. Miyamoto. *Plasma Physics for Nuclear Fusion*. The MIT Press, Cambridge, Massachusetts, revised edition, 1989.
- [25] K. C. Ng and W. L. Shen. Solution nebulization into a low-power argon microwave-induced plasma for atomic emission spectrometry: study of synthetic ocean water. *Anal. Chem.*, 58:2084–2087, 1986.
- [26] K. Ogura, H. Yamada, Y. Sato, and Y. Okamoto. Excitation temperature in high-power nitrogen microwave-induced plasma at atmospheric pressure. *Applied Spectroscopy*, 51(10):1496–1499, 1997.
- [27] M. Ohata and N. Furuta. Evaluation of the detection capability of a high power nitrogen microwave-induced plasma for both atomic emission and mass spectrometry. *J. of Analytical Atomic Spectrometry*, 13:447–453, May 1998.



- [28] Y. Okamoto. Annular-shaped microwave-induced nitrogen plasma at atmospheric pressure for emission spectrometry of solutions. *Analytical Sciences*, 7:283–288, April 1991.
- [29] OMEGA, Stamford, CT. *Industrial Rotameters FL1650/1660 Series*, 1995.
- [30] *Continuous Emission Monitors Subcommittee of Research Committee on Industrial and Municipal Waste*, Newark, NJ, 1994.
- [31] B. R. Pollack. Establishing isokinetic flow for a plasma torch exhaust gas diagnostic for a plasma hearth furnace. Master's thesis, Massachusetts Institute of Technology, Nuclear Engineering Department and Mechanical Engineering Department, 1996.
- [32] P. A. Rizzi. *Microwave Engineering Passive Circuits*. Printice Hall, Inc., Englewood Cliffs, New Jersey, 1988.
- [33] A. V. Timofeev. Theory of microwave discharges at atmospheric pressures. *Plasma Physics Reports*, 23(72):158–164, 1997.
- [34] P. P. Woskov, K. Hadidi, P. Thomas, K. Green, and G. Flores. Accurate and sensitive metals emissions monitoring with an atmospheric microwave plasma having a real-time span calibration. *Journal of Waste Management*. To be published in May, 2000.
- [35] A. T. Zander and G. M. Hieftje. Microwave-supported discharges. *Applied Spectroscopy*, 35(4):357–371, 1981.